

## Supporting Information

### Flexible Thiourea Linked Covalent Organic Frameworks

Baiwei Ma,<sup>a+</sup> Chunzhi Li,<sup>b+</sup> Lipeng Zhai,<sup>a\*</sup> Fujia Hu,<sup>a</sup> Yimeng Xu,<sup>a</sup> Huijie Qiao,<sup>a</sup> Zhuo Wang,<sup>a</sup> Wenying Ai,<sup>a</sup> Liwei Mi<sup>a\*</sup>

a: Henan Key Laboratory of Functional Salt Materials, Center for Advanced Materials Research, School of Material and Chemical Engineering, Zhongyuan University of Technology, Zhengzhou 450007 (P. R. China)

b: State Key Laboratory of Catalysis, Dalian Institute of Chemical Physics, Chinese Academy of Science, 457 Zhongshan Road, Dalian 116023 (P. R. China)

Email: zhailp@zut.edu.cn, mlwzzu@163.com

#### Contents

#### Section A. Materials and Methods

#### Section B. Supporting Figures

#### Section C. Supporting Tables

#### Section D. Supporting References

## Section A. Materials and Methods

$^1\text{H}$  NMR and  $^{13}\text{C}$  NMR spectra were measured on a Bruker 400 MHz spectrometer, while chemical shifts ( $\delta$  in ppm) were determined using a standard of the solvent residual proton. Solid state Fourier  $^{13}\text{C}$  NMR spectra were measured on a Bruker 400 MHz spectrometer. Transform infrared (FT IR) spectra were recorded on a JASCO model FT IR-6100 infrared spectrometer. X-ray diffraction (XRD) data were recorded on a Bruker D8 Focus Powder X-ray Diffractometer by using powder on glass substrate, from  $2\theta = 2^\circ$  up to  $30^\circ$  with  $0.01^\circ$  increment. Elemental analysis was performed on an Elementar vario MICRO cube elemental analyzer. TGA measurements were performed on a Discovery TGA under  $\text{N}_2$ , by heating from 30 to  $800^\circ\text{C}$  at a rate of  $10^\circ\text{C min}^{-1}$ . Nitrogen sorption isotherms were measured at 77 K with a TriStar II instrument (Micromeritics). The Brunauer-Emmett-Teller (BET) method was utilized to calculate the specific surface areas. By using the non-local density functional theory (NLDF) model, the pore volume was derived from the sorption curve. Morphology images were characterized with a Zeiss Merlin Compact field emission scanning electron microscope (FE-SEM) equipped with an energy-dispersive X-ray spectroscopy (EDS) system at an electric voltage of 5 KV. HRTEM images were obtained with a transmission electron microscope (TEM, FEI Tecnai G2) installed with an energy dispersive spectrometer (EDS, Oxford).

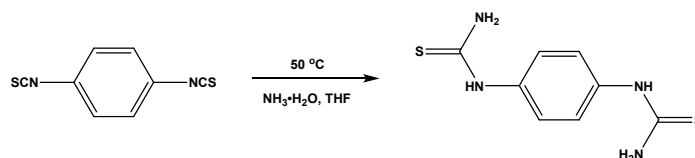
**Simulations.** The process of simulating COF structure was accomplished via Materials Studio software (version 8.0) of Accelrys Company. The hexagonal crystal system with P6 symmetry group was set as the initial AA stacking COFs structures. The cell parameters  $a$  and  $c$  were obtained from the calculation of experimental PXRD of COF by Bragg's law. After the smallest asymmetric unit was filled into the blank cell, the Forcite tools package was employed to optimize the cell geometry including energy minimization. The AB stacking structure was built with the similar process as described above, with the exception that a supercell with double  $c$  value was selected as the initial cell of staggered structure. The cell optimized from the universal force fields was subsequently refined using the Pawley refinement method in Reflex tools.<sup>[S1-S3]</sup>

**Stability test.** COF samples (20 mg) were kept for 24h at room temperature in HCl (1 M), and NaOH (1 M), respectively. The samples were collected by filtration and rinsed with water and THF several times. The COF were dried under vacuum at  $100^\circ\text{C}$  for 12 h and subjected to PXRD.

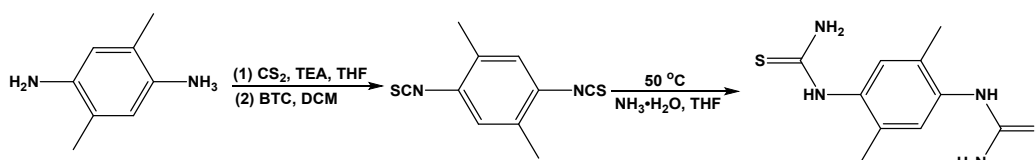
**Materials:** 1,4-Phenylene diisocyanate, anhydrous N-methyl-2-pyrrolidinone (NMP), 1,2,4-trichlorobenzene (TCB), triethylamine (TEA), and ammonium hydroxide (28–30%) were purchased from Sigma Aldrich. The acetic acid, 1,2-dichloromethane (DCM), N, N-diethylformamide (DEF), Tetrahydrofuran (THF), acetone and  $\text{CS}_2$  were purchased from Aladdin Chemicals. 1,3,5-Triformylphloroglucinol (TP) was purchased from Shanghai zhuogao new material Co., Ltd. 1,1'-(1,4-phenylene) bis(thiourea) (TU), 1,1'-(2,5-dimethyl-1,4-phenylene) bis(thiourea) (DMTU) and 1,1'-(3,3'-

dimethyl-[1,1'-biphenyl]-4,4'-diyl) bis(thiourea) (DMPTU) were prepared by ourselves, All the other solvents were purchased from Aladdin Chemicals and used as received without further purification.

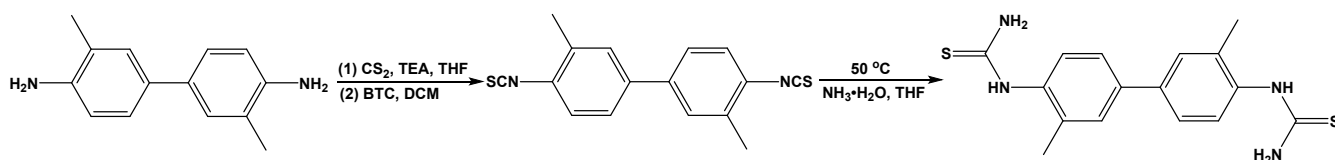
### Monomer synthesis:



**1,1'-(1,4-phenylene) bis(thiourea) (TU):** 1,4-diisothiocyanatobenzene (1 g) was added to a 20 mL ammonium hydroxide solution (28–30%) at room temperature, and a small amount of THF was added to the reaction system. The resulting reaction mixture was stirred at 50 °C for 2 hours. Then the reaction mixture was cooled to room temperature. The product was collected via filtration, washed with water (25 mL), THF (25 mL) and dried in vacuum at 50 °C in 90% yield. <sup>1</sup>H NMR (400 MHz, DMSO) δ 9.64 (s, 2H), 7.33 (s, 8H); <sup>13</sup>C NMR (100 MHz, DMSO) δ 181.49 (s, 1H), 136.00 (s, 1H), 124.24 (s, 3H); HRMS (ESI-TOF): Calcd for C<sub>8</sub>H<sub>10</sub>N<sub>4</sub>S<sub>2</sub>H<sup>+</sup>[M+H]<sup>+</sup> 227.0420, Found 227.0436.



**1,1'-(2,5-dimethyl-1,4-phenylene) bis(thiourea) (DMTU):** To 50 mL of THF was added 2,5-dimethylbenzene-1,4-diamine (20 mmol, 2.72 g), TEA (100 mmol, 13.9 mL) and CS<sub>2</sub> (100 mmol, 6 mL). The resulting reaction mixture was stirred for 12 hours at 40 °C. Then the yellow solid was collected via filtration and 50 mL of DCM was added, triphosgene (BTC, 40 mmol) in DCM was dropwise added at 0 °C. and the reaction proceeded for 4 hours at reflux temperature. The pure 1,4-diisothiocyanato-2,5-dimethylbenzene compound was obtained by flash chromatography on silica gel with PE as elution solvent in 8% yield. The resulting 1,4-diisothiocyanato-2,5-dimethylbenzene compound (0.5 g) was added to a 15 mL ammonium hydroxide solution (28–30%) at room temperature, and a small amount of THF was added to the reaction system. The resulting reaction mixture was stirred at 50 °C for 2 hours. Then the reaction mixture was cooled to room temperature. The product was collected via filtration, washed with water (20 mL), THF (20 mL) and dried in vacuum at 50 °C in 94% yield. <sup>1</sup>H NMR (600 MHz, DMSO) δ 9.30 (s, 2H), 7.72 (s, 2H), 7.02 (s, 2H), 6.52 (s, 2H), 2.11 (s, 6H); <sup>13</sup>C NMR (150 MHz, DMSO) δ 181.7, 135.7, 133.6, 130.2, 17.4. HRMS (ESI-TOF): Calcd for C<sub>10</sub>H<sub>14</sub>N<sub>4</sub>S<sub>2</sub>H<sup>+</sup>[M+H]<sup>+</sup> 255.0738, 255.0766.



**1,1'-(3,3'-dimethyl-[1,1'-biphenyl]-4,4'-diyl) bis(thiourea) (DMPTU):** To 50 mL of THF was added 3,3'-dimethyl-[1,1'-biphenyl]-4,4'-diamine (20 mmol, 4.24 g), TEA (100 mmol, 13.9 mL) and CS<sub>2</sub> (100 mmol, 6 mL). The resulting reaction mixture was stirred for 12 hours at 40 °C. Then the yellow solid was collected via filtration and 50 mL of DCM was added, triphosgene (BTC, 40 mmol) in DCM was dropwise added at 0 °C. Then, the reaction proceeded for 4 hours at reflux temperature. The pure 4,4'-diisothiocyanato-3,3'-dimethyl-1,1'-biphenyl compound was obtained by flash chromatography on silica gel with PE as elution solvent in 12% yield. The resulting compound (1 g) was added to a 20 mL ammonium hydroxide solution (28–30%) at room temperature, and a small amount of THF was added to the reaction system. The resulting reaction mixture was stirred at 50 °C for 2 hours. Then the reaction mixture was cooled to room temperature. The bithiourea product was collected via filtration, washed with water (30 mL), THF (30 mL) and petroleum ether (20 mL) and dried in vacuum at 50 °C in 92% yield. <sup>1</sup>H NMR (600 MHz, DMSO) δ 9.23 (s, 2H), 7.59 (s, 2H), 7.55 (d, *J* = 1.8 Hz, 2H), 7.47 (dd, *J* = 8.4, 1.8 Hz, 2H), 7.31 (d, *J* = 8.4 Hz, 2H), 7.03 (s, 2H), 2.26 (s, 6H); <sup>13</sup>C NMR (150 MHz, DMSO) δ 182.1, 138.1, 137.0, 135.1, 129.0, 128.3, 124.8, 18.2. HRMS (ESI-TOF): Calcd for C<sub>16</sub>H<sub>18</sub>N<sub>4</sub>S<sub>2</sub>H<sup>+</sup>[M+H]<sup>+</sup> 331.1051, 331.1064.

**Synthesis of TP-TU-COF:** A pyrex tube (10 ml) is charged with 1,3,5-Triformylphloroglucinol (20 mg), 1,1'-(1,4-phenylene) bis(thiourea) (32.2 mg), 0.6 mL NMP, 0.4 mL TCB and 0.1 mL of 6 M aqueous acetic acid. The tube was then flash frozen at 77 K and degassed by three freeze-pump-thaw cycles. The tube was sealed off and then heated at 150 °C for 3 days. The collected powder was washed with dimethylacetamide, tetrahydrofuran and acetone and dried at 100 °C under vacuum for 24 hours to get corresponding dark red powder in 82% isolated yield.

**Synthesis of TP-DMTU-COF:** A pyrex tube (10 ml) is charged with 1,3,5-Triformylphloroglucinol (20 mg), 1,1'-(2,5-dimethyl-1,4-phenylene) bis(thiourea) (36.2 mg), 0.6 mL NMP, 0.4 mL TCB and 0.1 mL of 6 M aqueous acetic acid. The tube was then flash frozen at 77 K and degassed by three freeze-pump-thaw cycles. The tube was sealed off and then heated at 150 °C for 3 days. The collected powder was washed with dimethylacetamide, tetrahydrofuran and acetone and dried at 100 °C under vacuum for 24 hours to get corresponding red powder in 87% isolated yield.

**Synthesis of TP-DMPTU-COF:** A pyrex tube (10 ml) is charged with 1,3,5-Triformylphloroglucinol (20 mg), 1,1'-(3,3'-dimethyl-[1,1'-biphenyl]-4,4'-diyl) bis(thiourea) (47.0 mg), 0.6 mL NMP, 0.4 mL TCB and 0.1 mL of 6 M aqueous acetic acid. The tube was then flash frozen at 77 K and degassed by three freeze-pump-thaw cycles. The tube was sealed off and then heated at 150 °C for 3 days. The

collected powder was washed with dimethylacetamide, tetrahydrofuran and acetone and dried at 100 °C under vacuum for 24 hours to get corresponding dark red powder in 89% isolated yield.

**The procedure of Knoevenagel reaction about aldehydes and malononitrile:** A reaction ground tube (10 ml) is charged with COF catalyst (2 mol%), aldehydes (0.3 mmol), malononitrile (0.3 mmol), toluene (2 mL) and H<sub>2</sub>O (0.4 mL). After being stirred at 60 °C for 10 h, the solvent was removed and the pure product was obtained by flash chromatography on silica gel.

## Section B. Supporting Figures

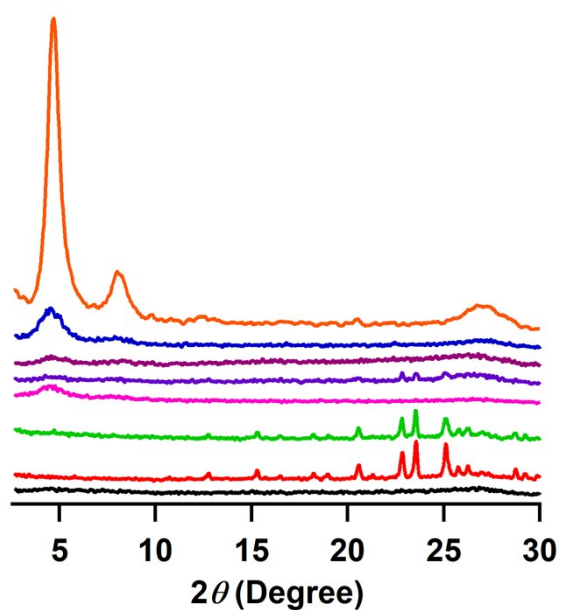


**Figure S1.** XRD profiles of the TP-TU-COF synthesized under different conditions. black: NMP/TCB/6 M AcOH ( 4:6:1 by vol., 90 °C); red: NMP/TCB/6 M AcOH ( 2:8:1 by vol., 90 °C); green: n-BuOH/TCB/6 M AcOH ( 5:5:1 by vol., 90 °C); pink: NMP/TCB/6 M AcOH ( 4:6:1 by vol., 120 °C); violet: NMP/TCB/6 M AcOH ( 2:8:1 by vol., 120 °C); purple: NMP/TCB/6 M AcOH ( 6:4:1 by vol., 180 °C); blue: NMP/TCB/6 M AcOH ( 6:4:1 by vol., 120 °C); orange: NMP/TCB/6 M AcOH ( 6:4:1 by vol., 150 °C).

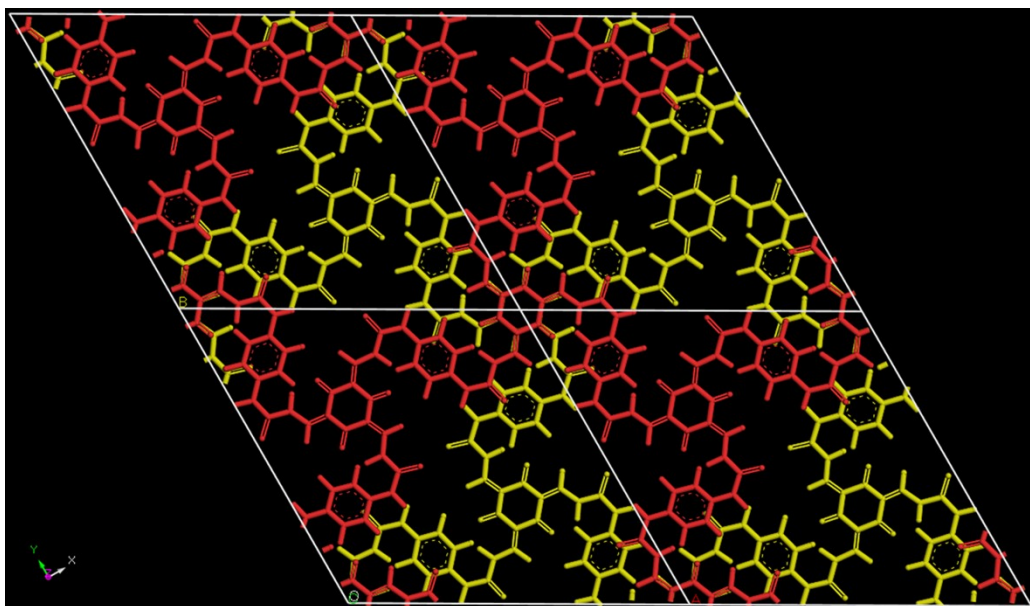


**Figure S2.** Reproduced AB stacking crystal structure of TP-TU-COF.

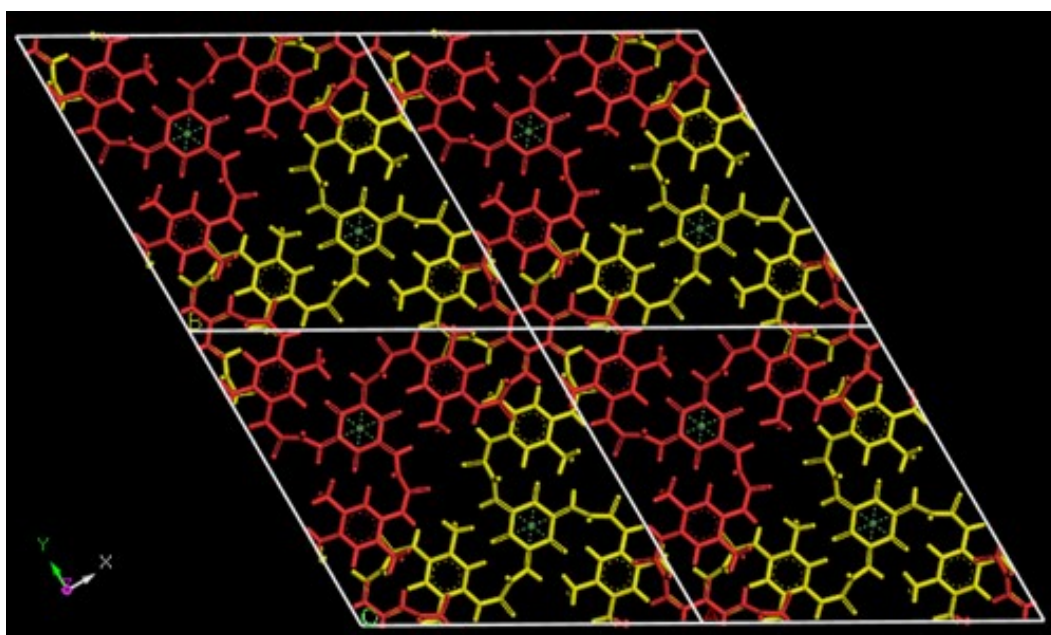


**Figure S3.** Reproduced AB stacking crystal structure of TP-DMTU-COF.

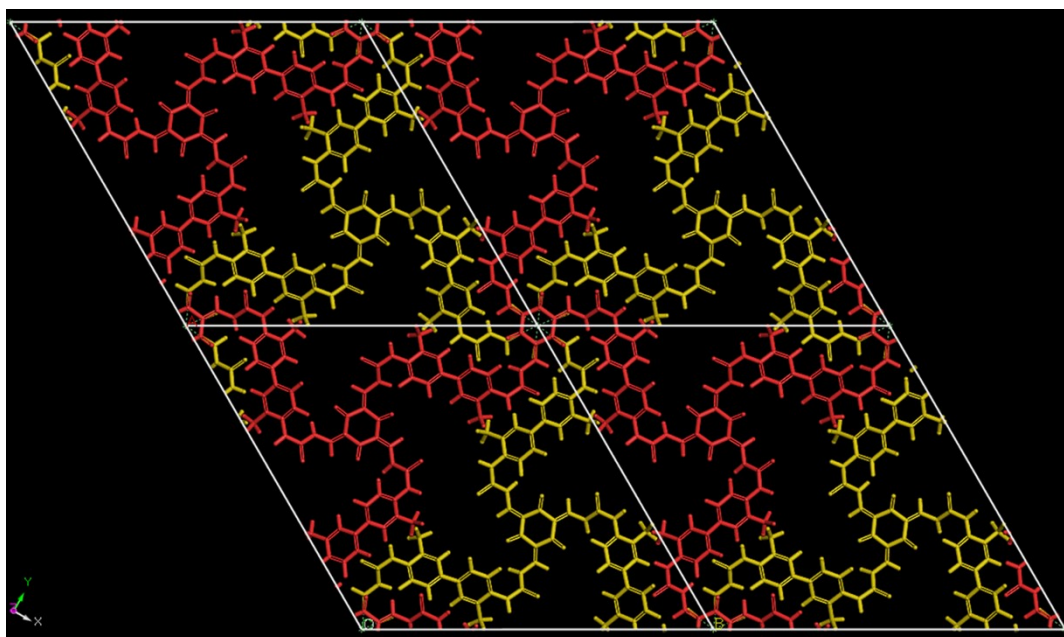


**Figure S4.** Reproduced AB stacking crystal structure of TP-DMPTU-COF.



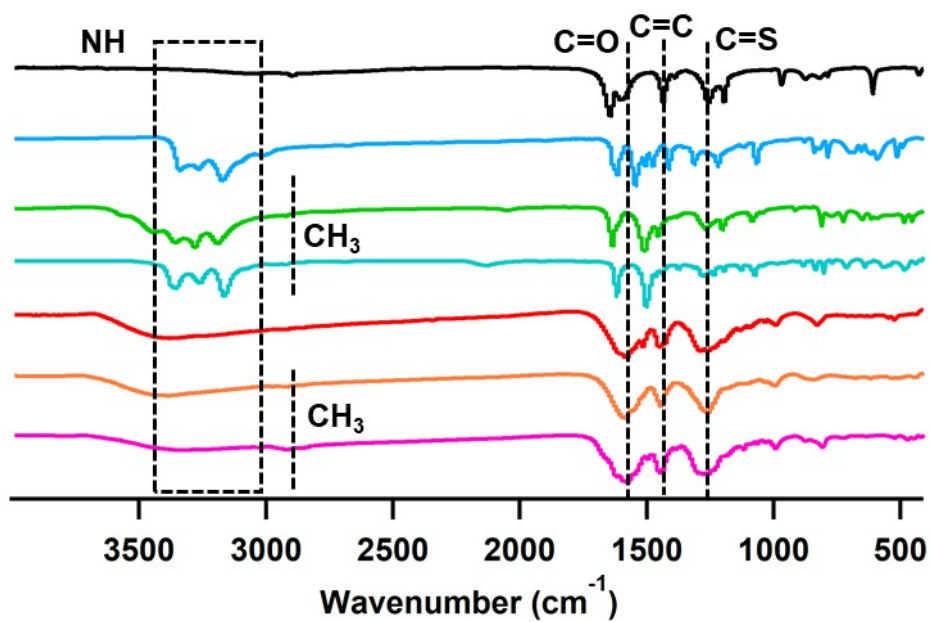


**Figure S5.** FT-IR spectra of (red) TP-TU-COF, (orange) TP-DMTU-COF, and (pink) TP-DMPTU-COF and corresponding monomers (black) TP, (blue) TU, (green) DMTU, and (dark green).

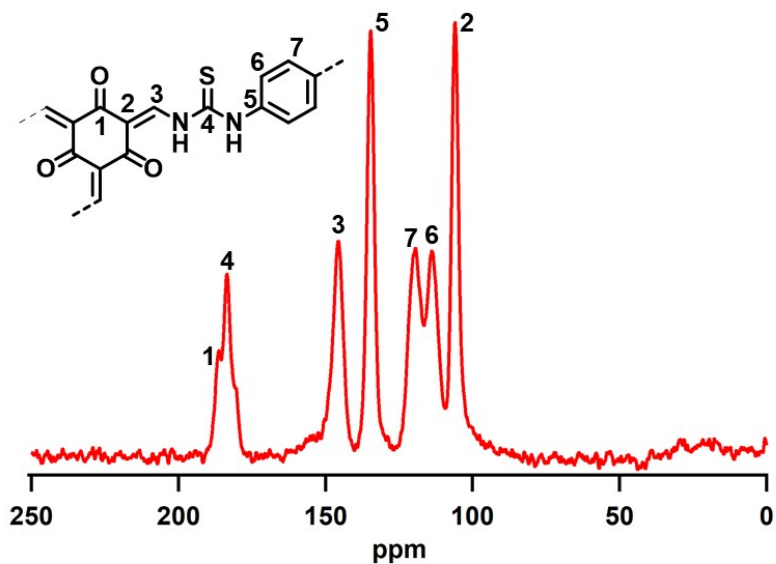


**Figure S6.**  $^{13}\text{C}$  CP/MAS solid-state NMR spectra of TP-TU-COF.

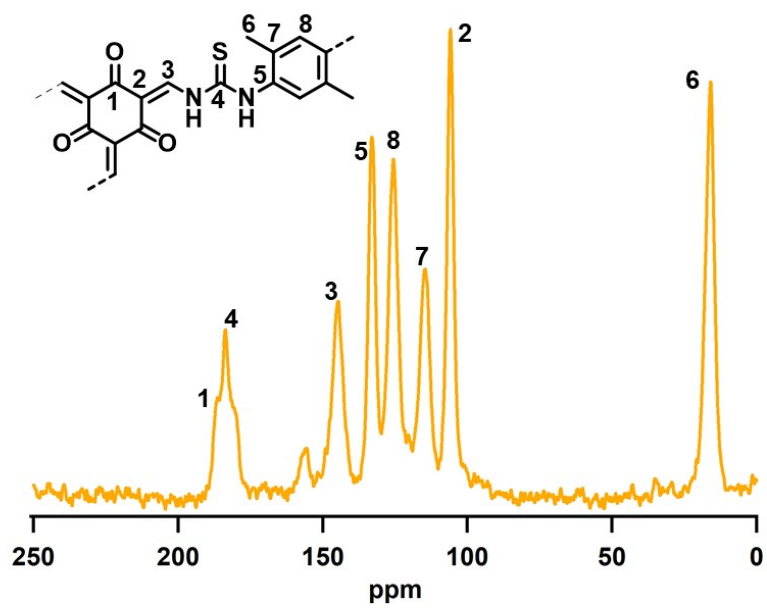


**Figure S7.**  $^{13}\text{C}$  CP/MAS solid-state NMR spectra of TP-DMTU-COF.

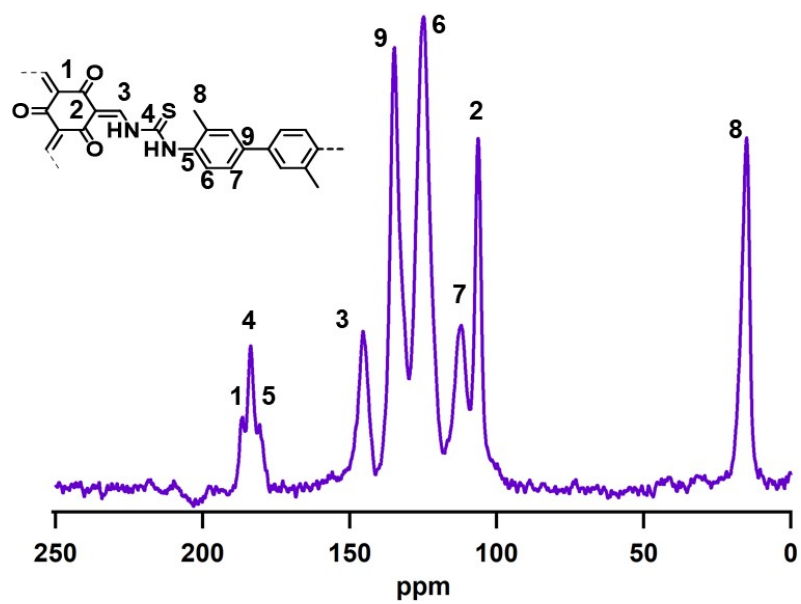


**Figure S8.**  $^{13}\text{C}$  CP/MAS solid-state NMR spectra of TP-DMPTU-COF.

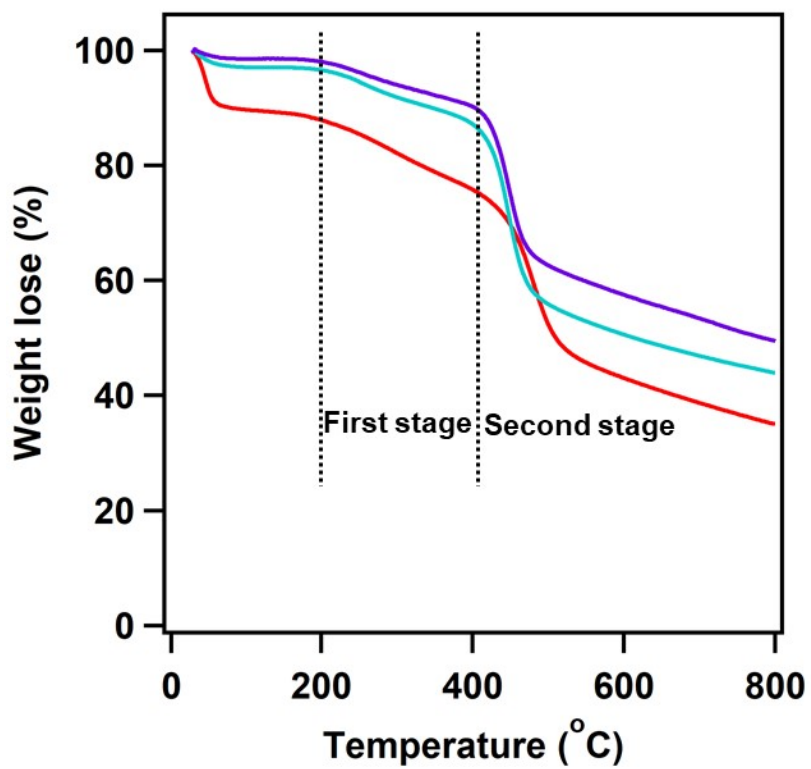


**Figure S9.** Thermogravimetric curves of (red) TP-TU-COF, (green) TP-DMTU-COF, and (purple) TP-DMPTU-COF.

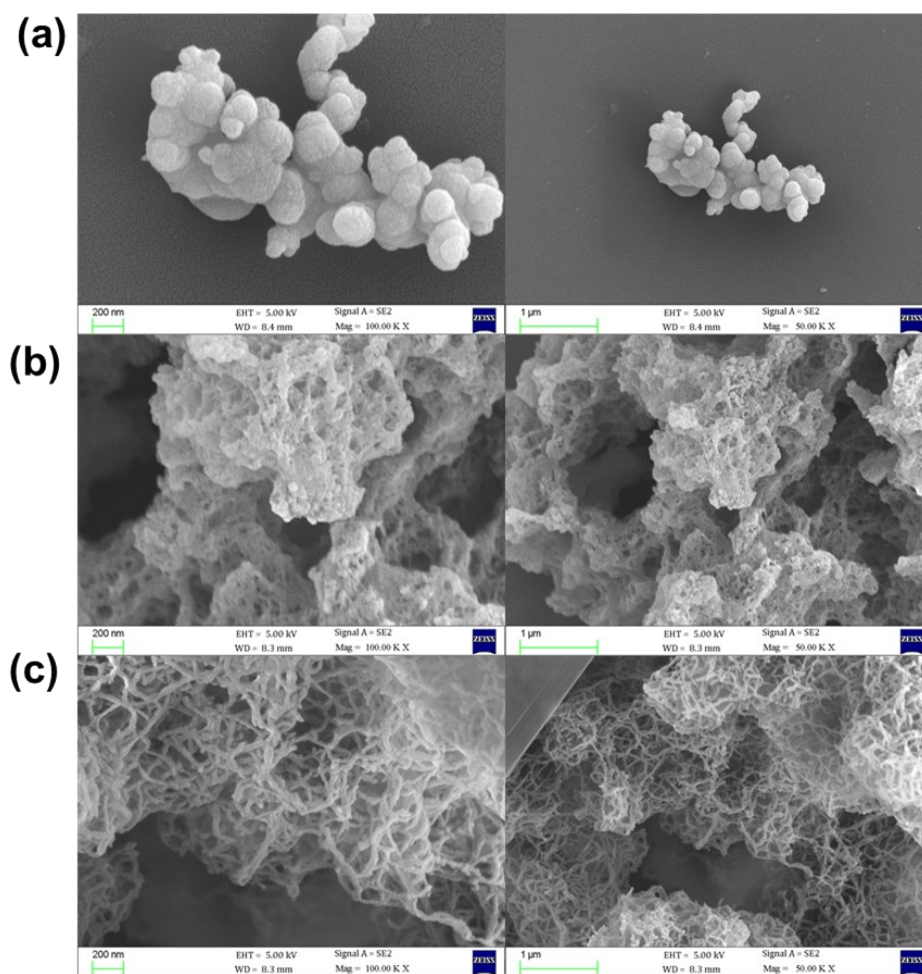


**Figure S10.** SEM images of (a) TP-TU-COF, (b) TP-DMTU-COF, and (c) TP-DMPTU-COF.

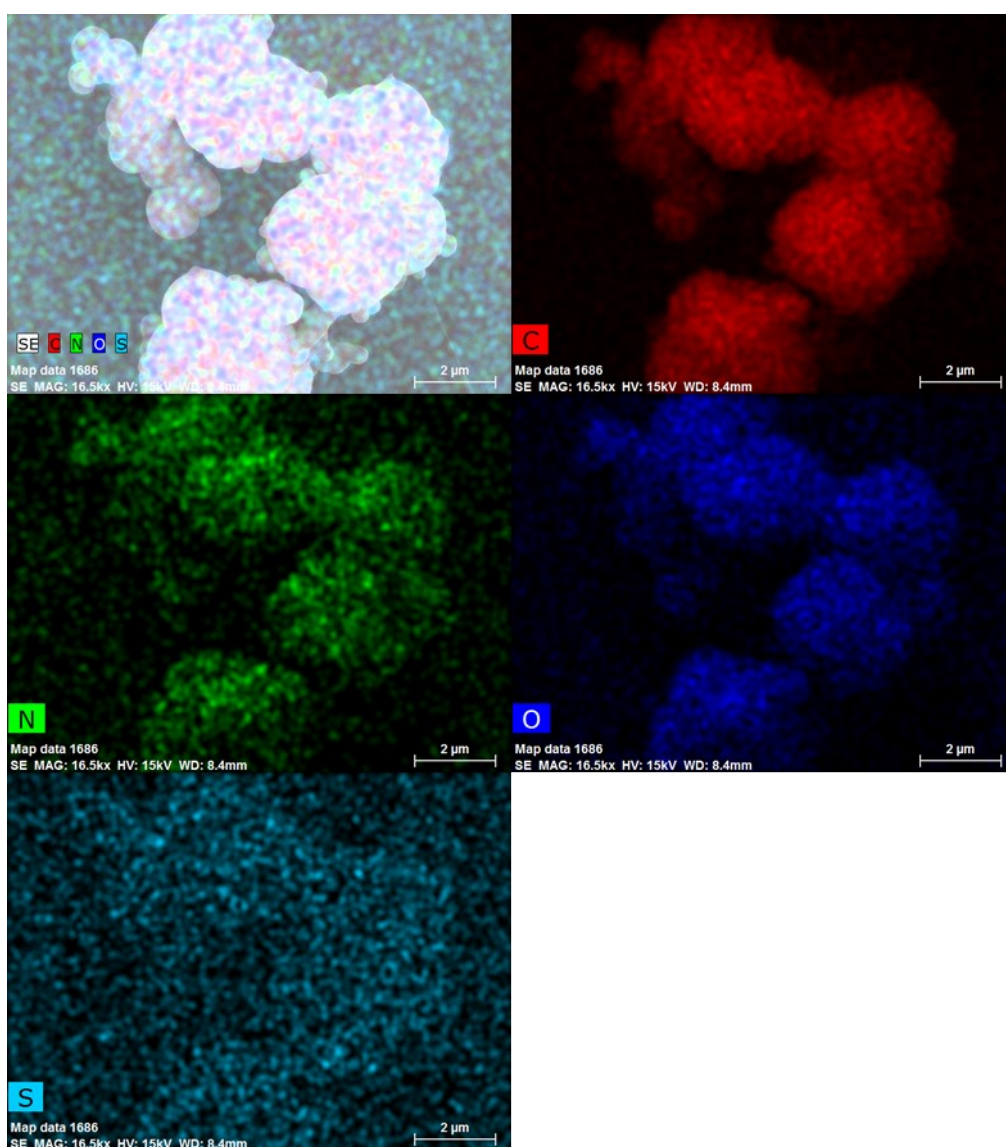


**Figure S11.** Elemental distribution mapping of TP-TU-COF.



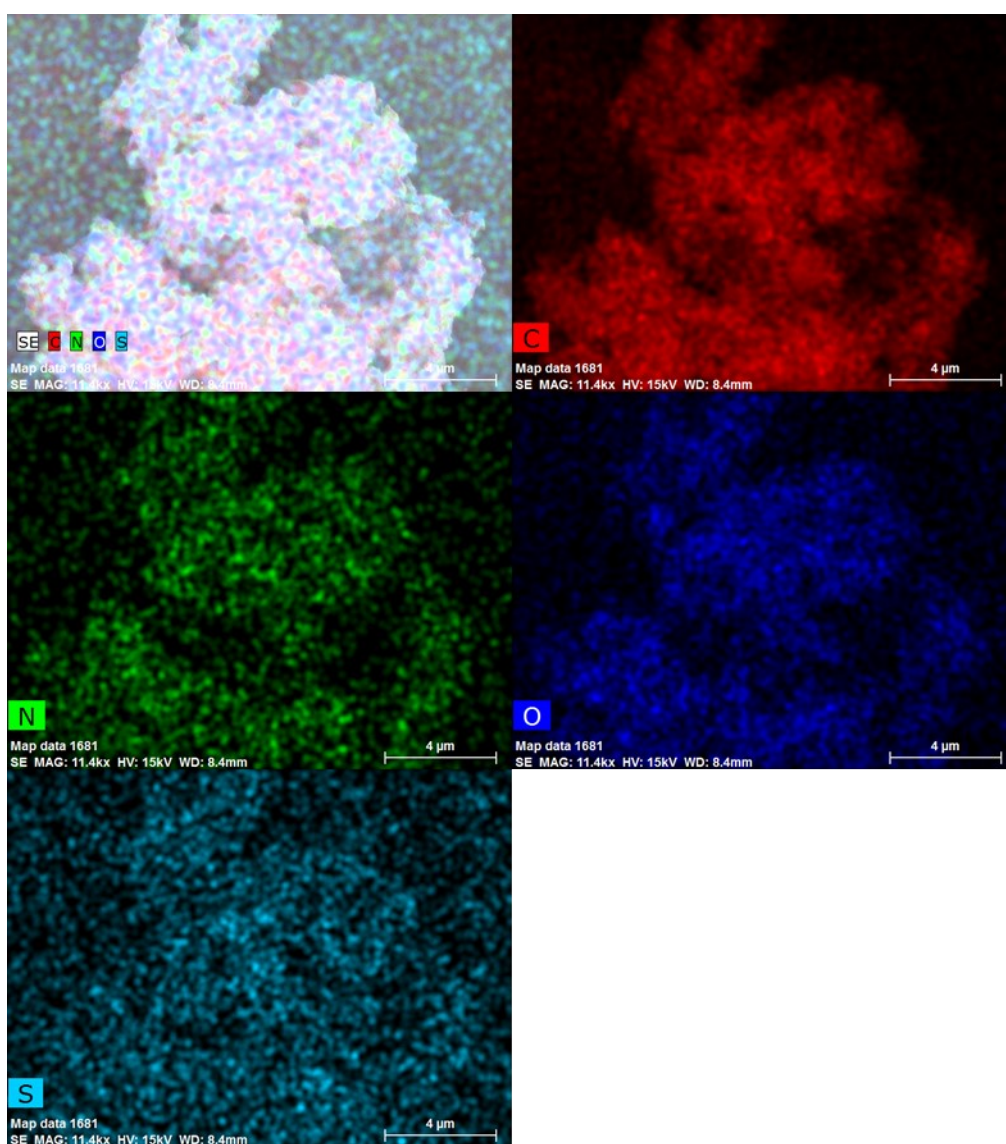


**Figure S12.** Elemental distribution mapping of TP-DMTU-COF.

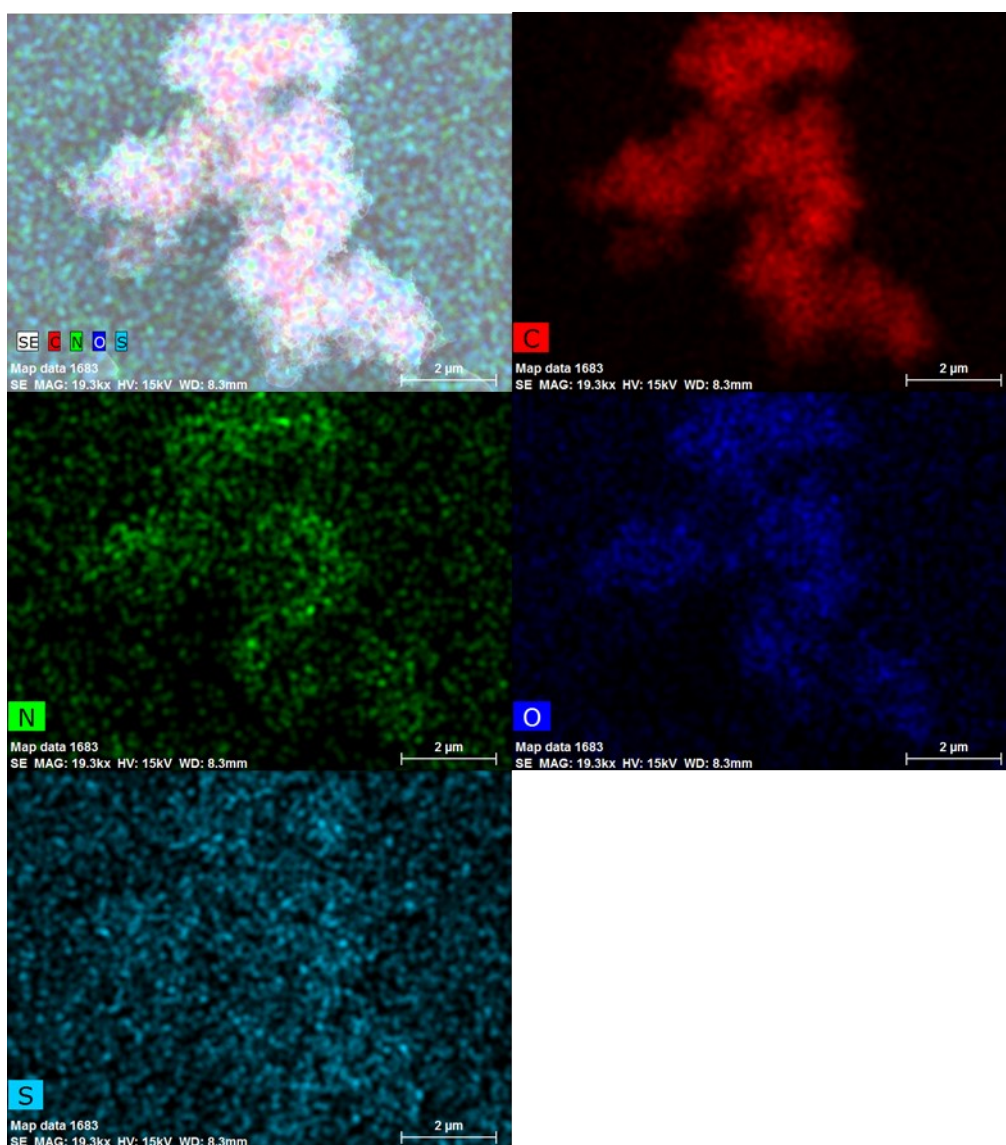


**Figure S13.** Elemental distribution mapping of TP-DMPTU-COF.



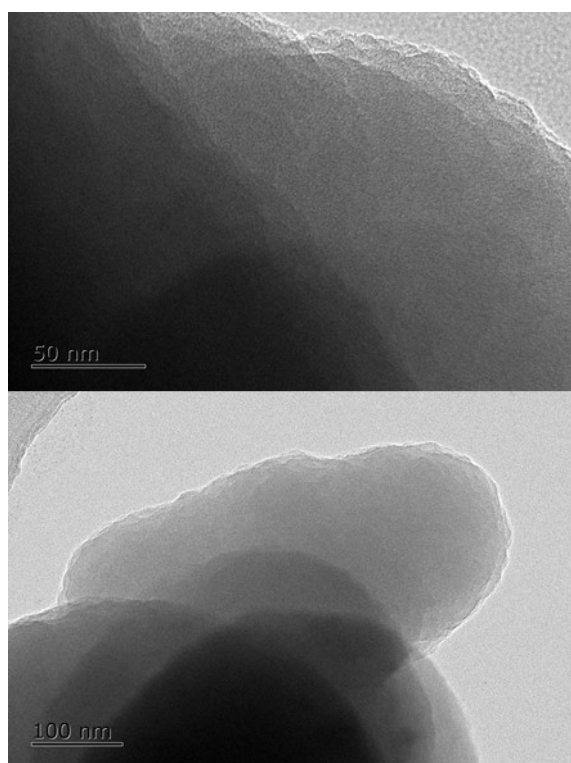


**Figure S14.** TEM images of TP-TU-COF.

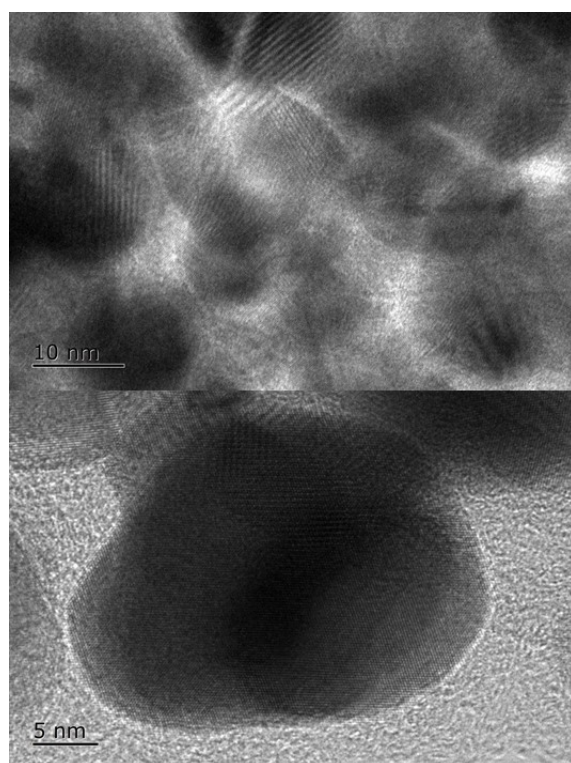


**Figure S15.** TEM images of TP-DMTU-COF.

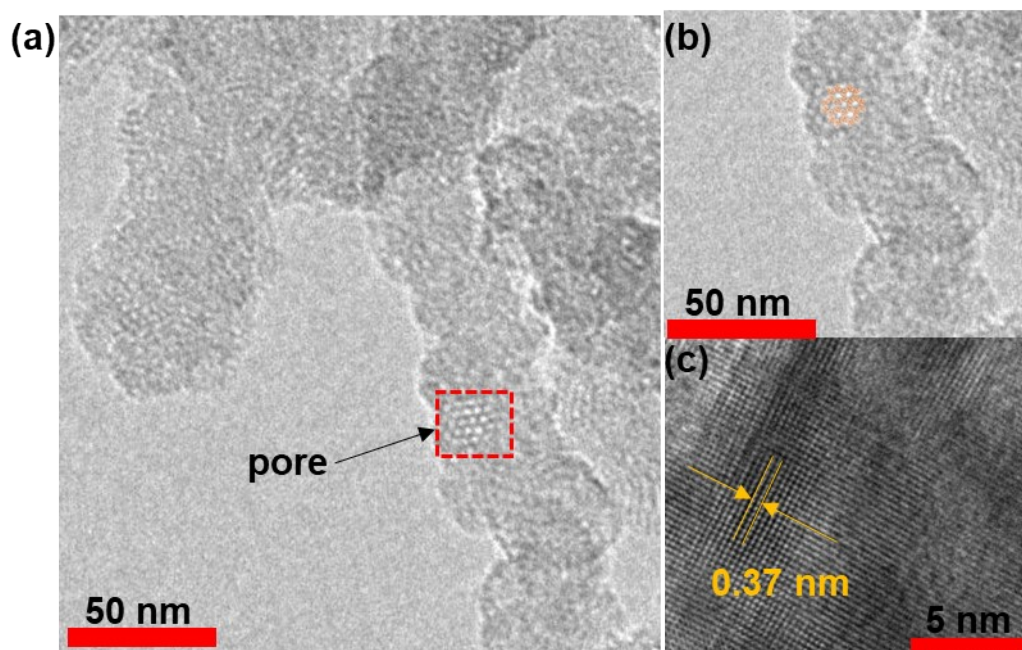


**Figure S16.** TEM images of TP-DMPTU-COF: (a, b) hexagonal pores, TEM image of TP-DMPTU-COF showing hexagonal pores viewing from [001] direction, and (c) layer distance.

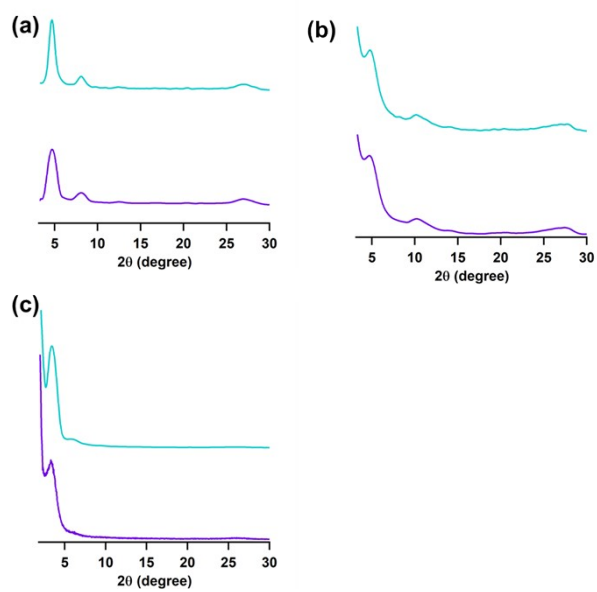


**Figure S17.** Chemical stability: PXRD profiles of (a) TP-TU-COF, (b) TP-DMTU-COF, and (c) TP-DMPTU-COF after treatment in HCl (1M, blue) and NaOH (1M, purple).

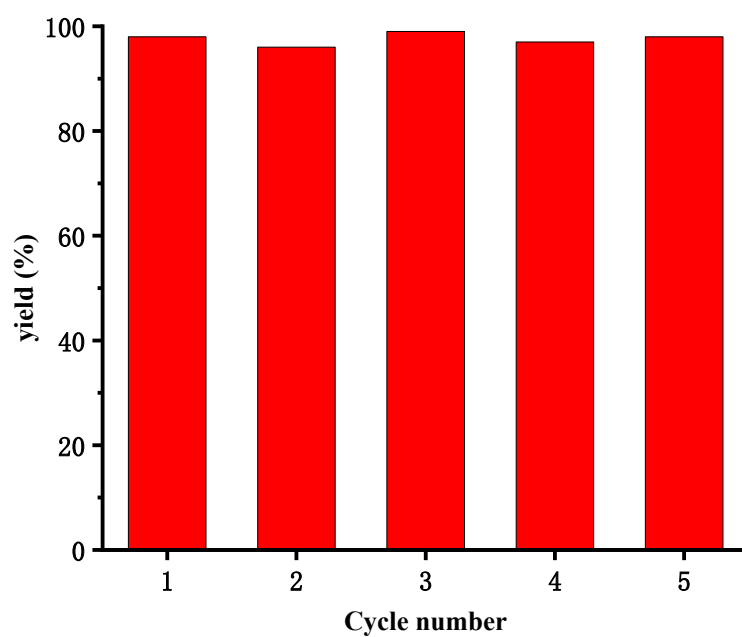


**Figure S18.** Catalytic activity performance of TP-DMPTU-COF for catalyzing compound 1a for five cycles.

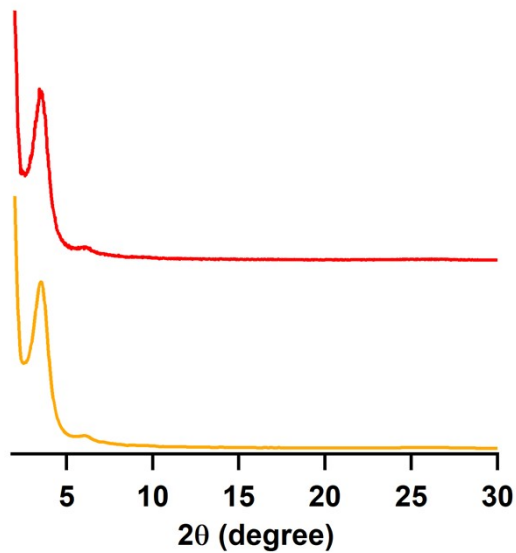
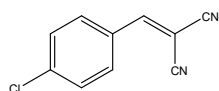
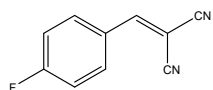


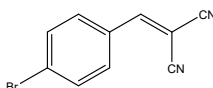
**Figure S19.** PXRD patterns of TP-DMPTU-COF before (red) and after (yellow) catalytic recycle performance.



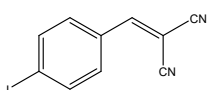
**2-(4-chlorobenzylidene)malononitrile(2a):** White solid; 97% yield;  $^1\text{H}$  NMR (600 MHz, DMSO)  $\delta$  8.54 (s, 1H), 8.02-7.90 (m, 2H), 7.77-7.66 (m, 2H);  $^{13}\text{C}$  NMR (150 MHz, DMSO)  $\delta$  160.6, 139.5, 132.6, 130.6, 130.2, 114.6, 113.5, 82.8.



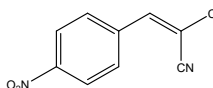
**2-(4-fluorobenzylidene)malononitrile(2b):** White solid; 92% yield;  $^1\text{H}$  NMR (600 MHz,  $\text{CDCl}_3$ )  $\delta$  7.97–7.94 (m, 2H), 7.74 (s, 1H), 7.32–7.16 (m, 2H);  $^{13}\text{C}$  NMR (150 MHz,  $\text{CDCl}_3$ )  $\delta$  166.1 (d,  $J = 259.5$  Hz), 158.3, 133.4 (d,  $J = 10.5$  Hz), 127.3, 117.2 (d,  $J = 22.5$  Hz), 113.5, 112.5, 82.4.



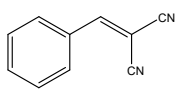
**2-(4-bromobenzylidene)malononitrile(2c):** White solid; 95% yield;  $^1\text{H}$  NMR (600 MHz,  $\text{CDCl}_3$ )  $\delta$  7.77 (d,  $J = 8.4$  Hz, 2H), 7.72 (s, 1H), 7.68 (d,  $J = 8.4$  Hz, 2H);  $^{13}\text{C}$  NMR (150 MHz,  $\text{CDCl}_3$ )  $\delta$  158.4, 133.1, 131.8, 129.9, 129.6, 113.4, 112.3, 83.5.



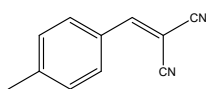
**2-(4-iodobenzylidene)malononitrile(2d):** White solid; 97% yield;  $^1\text{H}$  NMR (600 MHz,  $\text{CDCl}_3$ )  $\delta$  7.91 (d,  $J = 8.4$  Hz, 2H), 7.70 (s, 1H), 7.61 (d,  $J = 8.4$  Hz, 2H);  $^{13}\text{C}$  NMR (150 MHz,  $\text{CDCl}_3$ )  $\delta$  158.7, 139.0, 131.5, 130.1, 113.4, 112.3, 102.8, 83.5



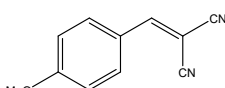
**2-(4-nitrobenzylidene)malononitrile(2e):** White solid; 89% yield;  $^1\text{H}$  NMR (600 MHz,  $\text{CDCl}_3$ )  $\delta$  8.39 (d,  $J = 9.0$  Hz, 2H), 8.08 (d,  $J = 9.0$  Hz, 2H), 7.89 (s, 1H);  $^{13}\text{C}$  NMR (150 MHz,  $\text{CDCl}_3$ )  $\delta$  156.8, 150.3, 135.8, 131.3, 124.6, 112.6, 111.6, 87.5.



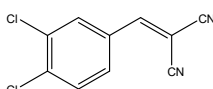
**benzylidenemalononitrile(2f):** White solid; 99% yield;  $^1\text{H}$  NMR (600 MHz,  $\text{CDCl}_3$ )  $\delta$  7.89 (d,  $J = 7.8$  Hz, 2H), 7.76 (s, 1H), 7.62 (t,  $J = 7.5$  Hz, 1H), 7.52 (t,  $J = 7.8$  Hz, 2H);  $^{13}\text{C}$  NMR (150 MHz,  $\text{CDCl}_3$ )  $\delta$  159.9, 134.6, 130.9, 130.7, 129.6, 113.7, 112.5, 82.8.



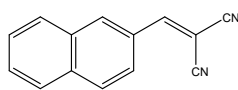
**2-(4-methylbenzylidene)malononitrile(2g):** White solid; 98% yield;  $^1\text{H}$  NMR (600 MHz,  $\text{CDCl}_3$ )  $\delta$  7.81 (d,  $J = 7.8$  Hz, 2H), 7.71 (s, 1H), 7.33 (d,  $J = 7.8$  Hz, 2H), 2.45 (s, 3H);  $^{13}\text{C}$  NMR (150 MHz,  $\text{CDCl}_3$ )  $\delta$  159.7, 146.4, 130.9, 130.4, 128.4, 114.0, 112.8, 81.2, 22.0.



**2-(4-methoxybenzylidene)malononitrile(2h):** White solid; 95% yield;  $^1\text{H}$  NMR (600 MHz,  $\text{CDCl}_3$ )  $\delta$  7.93–7.90 (m, 2H), 7.65 (s, 1H), 7.03–7.00 (m, 2H), 3.92 (s, 3H);  $^{13}\text{C}$  NMR (150 MHz,  $\text{CDCl}_3$ )  $\delta$  164.8, 158.9, 133.4, 124.0, 115.1, 114.4, 113.3, 99.9, 78.5, 55.8.

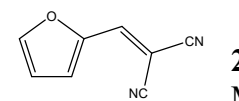


**2-(3,4-dichlorobenzylidene)malononitrile(2i):** White solid; 97% yield;  $^1\text{H}$  NMR (600 MHz,  $\text{CDCl}_3$ )  $\delta$  7.92 (d,  $J = 1.8$  Hz, 1H), 7.80 (dd,  $J = 8.4, 1.8$  Hz, 1H), 7.68 (s, 1H), 7.62 (d,  $J = 8.4$  Hz, 1H);  $^{13}\text{C}$  NMR (151 MHz,  $\text{CDCl}_3$ )  $\delta$  156.93 (s, 3H), 139.19 (s, 1H), 134.40 (s, 1H), 132.29 (s, 4H), 131.75 (s, 3H), 130.43 (s, 1H), 128.95 (s, 3H), 113.0, 111.9, 84.8.



**2-(naphthalen-2-ylmethylene)malononitrile(2j):** Yellow green solid; 85% yield;  $^1\text{H}$  NMR (600 MHz,  $\text{CDCl}_3$ )  $\delta$  8.27 (s, 1H), 8.06 (dd,  $J = 8.4, 1.8$  Hz, 1H), 7.96-7.93 (m, 2H), 7.90 (d,  $J = 8.4$  Hz, 2H), 7.88 (s, 1H), 7.68 (t,  $J = 7.5$  Hz, 1H), 7.61 (t,  $J = 7.5$  Hz, 1H);  $^{13}\text{C}$  NMR (150 MHz,  $\text{CDCl}_3$ )  $\delta$  159.7, 135.9, 134.5, 132.6, 130.0, 129.7, 128.5, 128.0, 127.7, 124.2, 114.0, 112.8, 82.2.

**2-((2,3-dihydrobenzo[b][1,4]dioxin-6-yl)methylene)malonitrile(2k):** Yellow solid; 96% yield; <sup>1</sup>H NMR (600 MHz, CDCl<sub>3</sub>) δ 7.57 (s, 1H), 7.50 (d, *J* = 1.8 Hz, 1H), 7.42 (dd, *J* = 9.0, 2.4 Hz, 1H), 6.96 (d, *J* = 9.0 Hz, 1H), 4.36-4.35 (m, 2H), 4.30-4.28 (m, 2H); <sup>13</sup>C NMR (150 MHz, CDCl<sub>3</sub>) δ 158.8, 149.7, 144.0, 125.9, 124.6, 119.6, 118.4, 114.3, 113.1, 79.2, 64.9, 64.0.



**2-(furan-2-ylmethylene) malonitrile(2l):** Yellow solid; 99% yield; <sup>1</sup>H NMR (600 MHz, CDCl<sub>3</sub>) δ 7.82 (d, *J* = 1.6 Hz, 1H), 7.53 (s, 1H), 7.37 (d, *J* = 3.6 Hz, 1H), 6.73 (dd, *J* = 3.6, 1.8 Hz, 1H); <sup>13</sup>C NMR (150 MHz, CDCl<sub>3</sub>) δ 149.6, 148.1, 143.1, 123.5, 114.4, 113.8, 112.6.

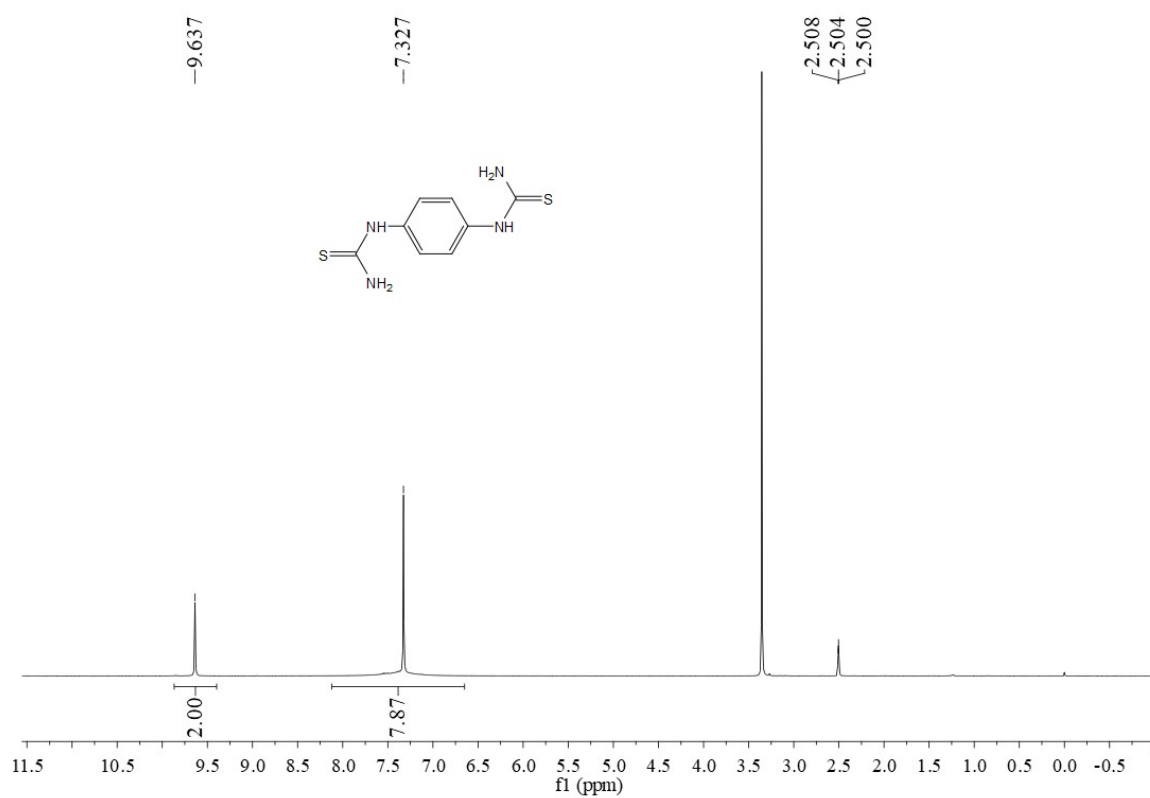


Figure S18. <sup>1</sup>H-NMR spectrum of TU.

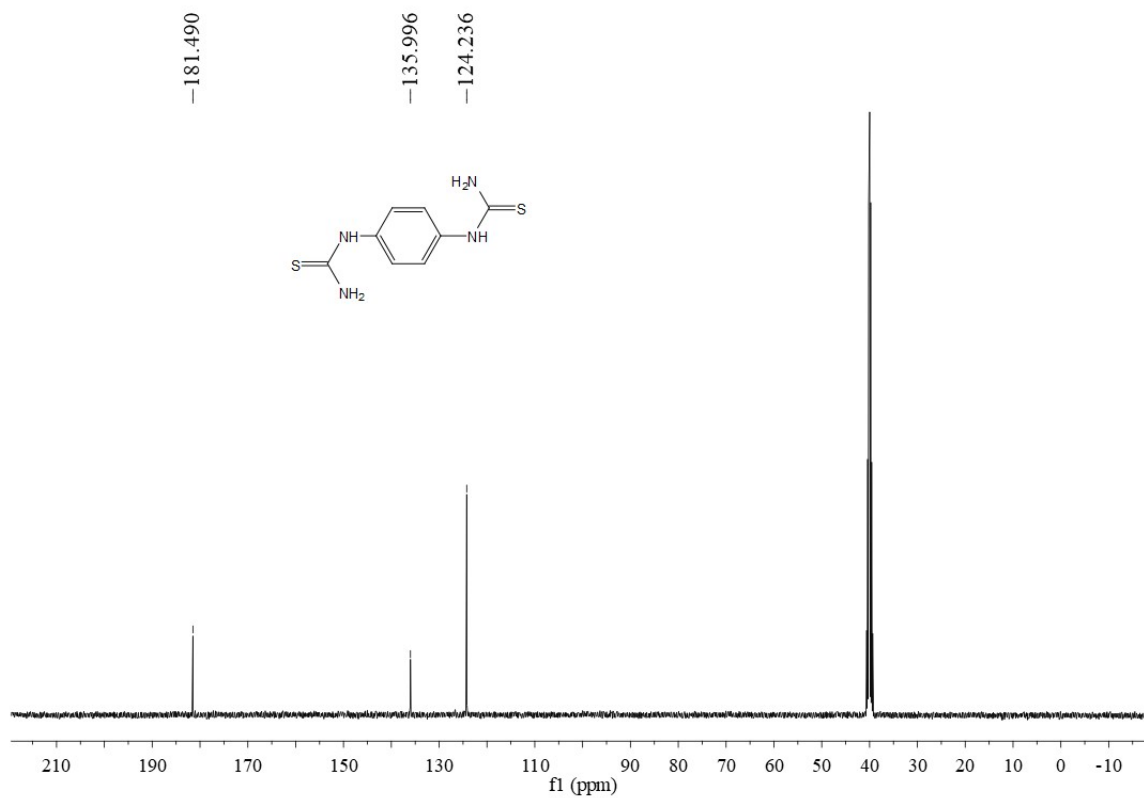


Figure S19. <sup>13</sup>C-NMR spectrum of TU.



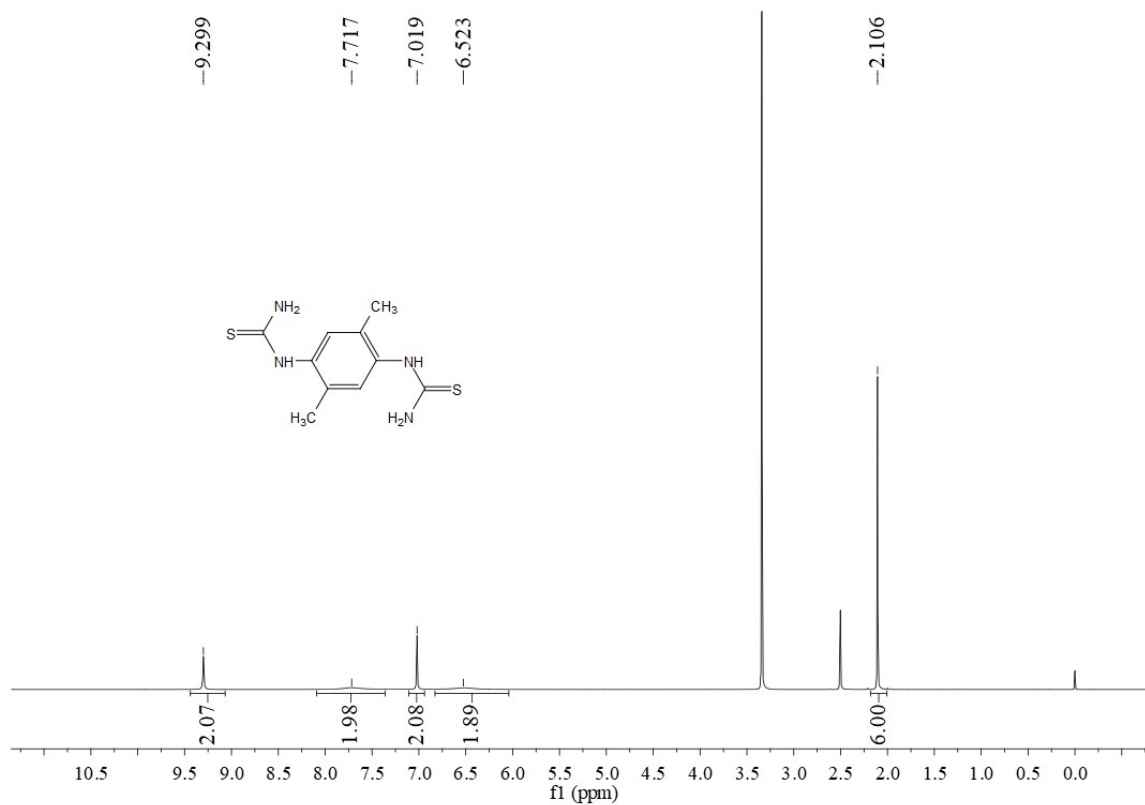


Figure S20. <sup>1</sup>H-NMR spectrum of DMTU.

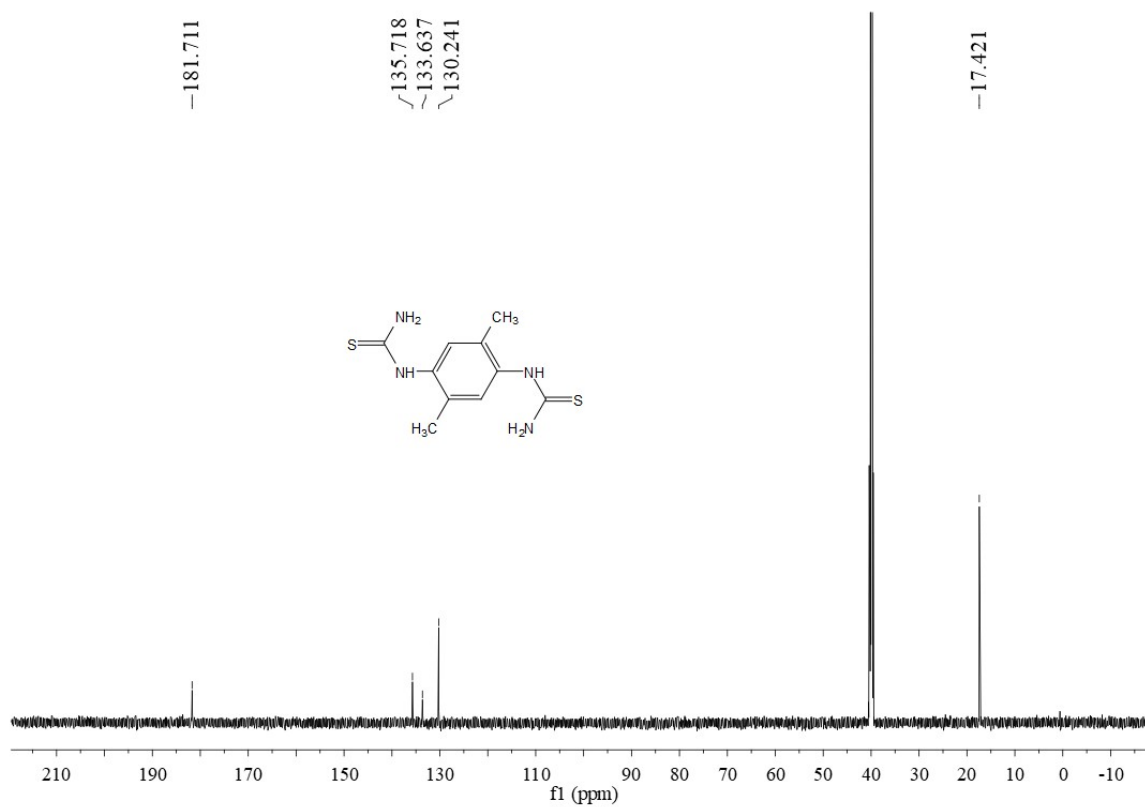


Figure S21. <sup>13</sup>C-NMR spectrum of DMTU.

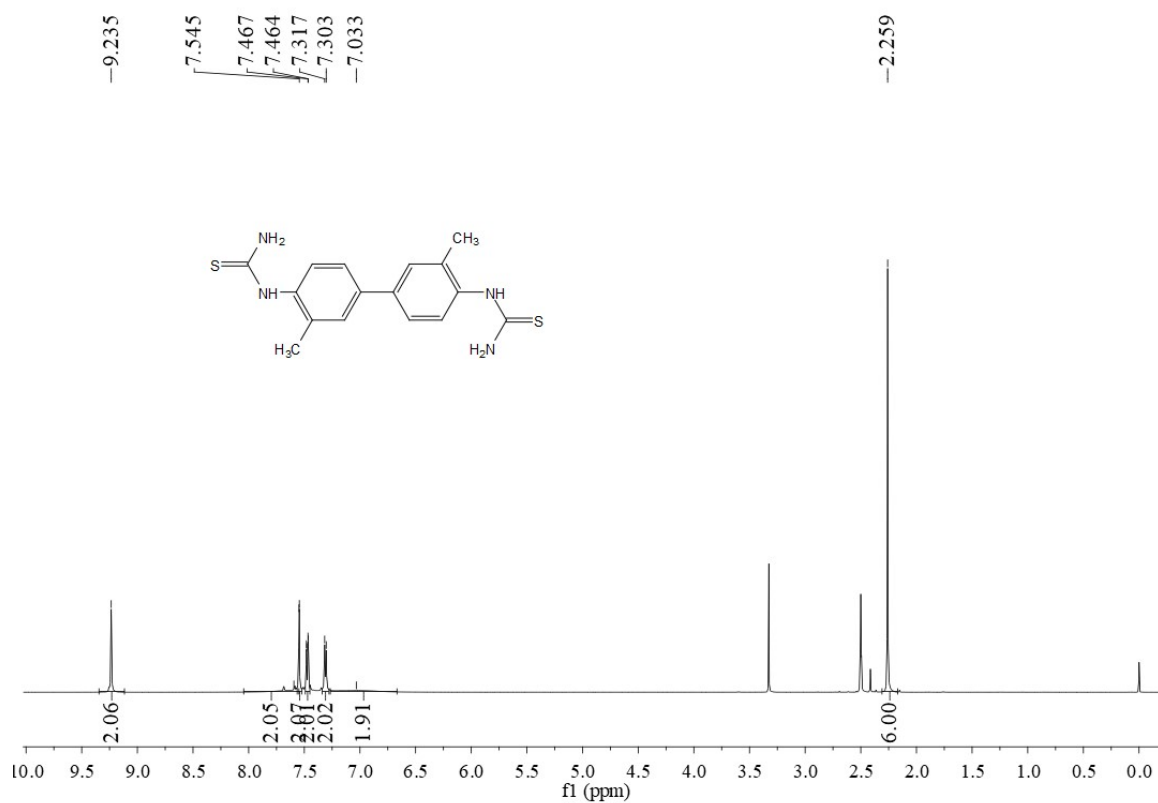


Figure S22. <sup>1</sup>H-NMR spectrum of DMPTU.

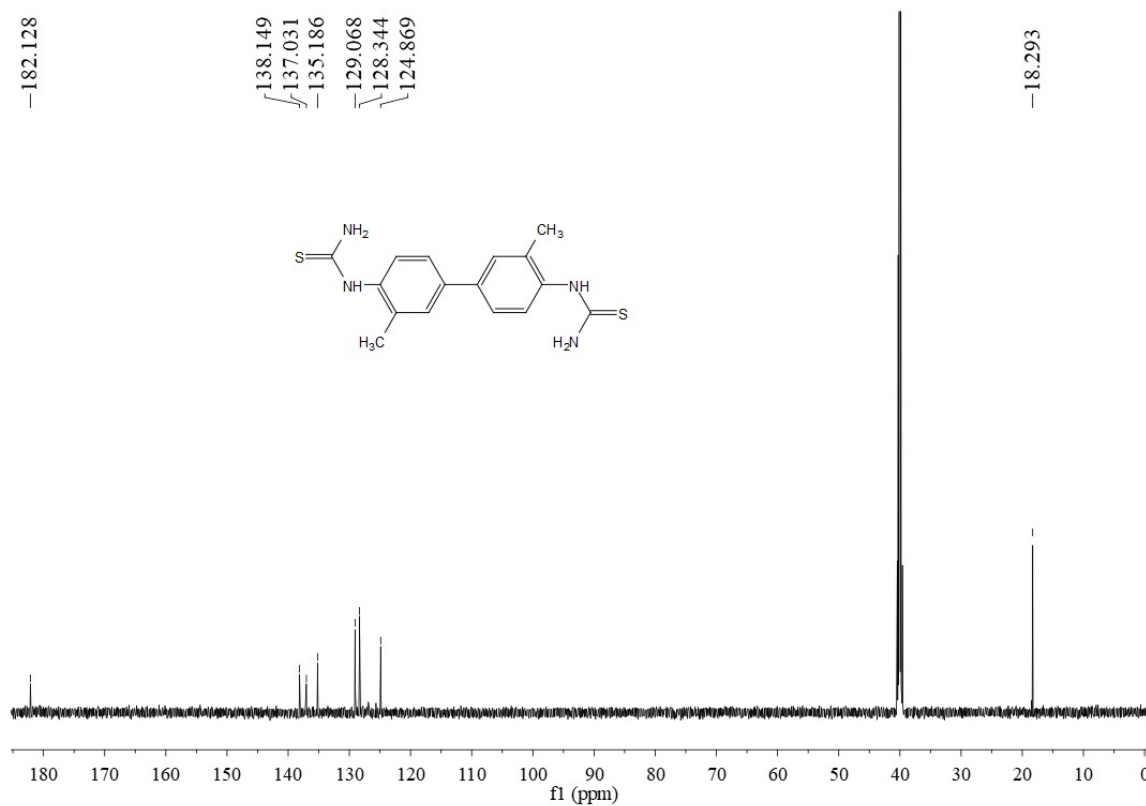


Figure S23. <sup>13</sup>C-NMR spectrum of DMPTU.

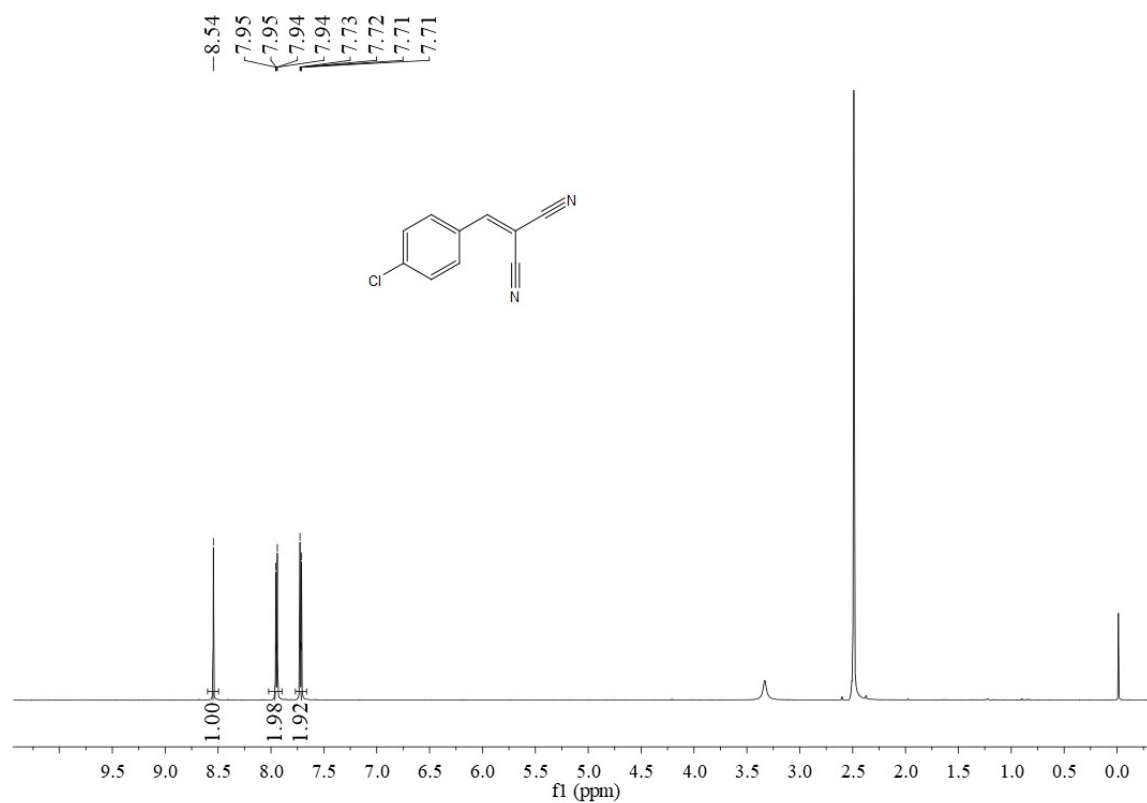


Figure S24. <sup>1</sup>H-NMR spectrum of 2a.

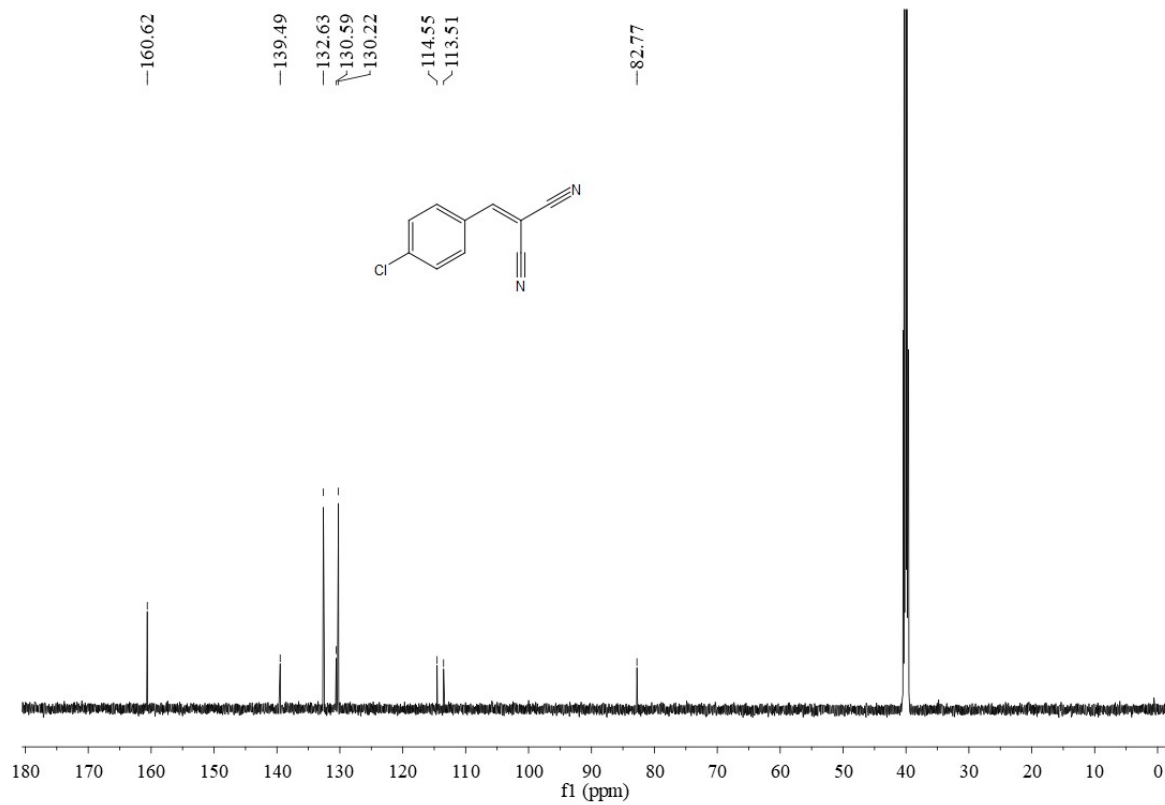


Figure S25. <sup>13</sup>C-NMR spectrum of 2a.

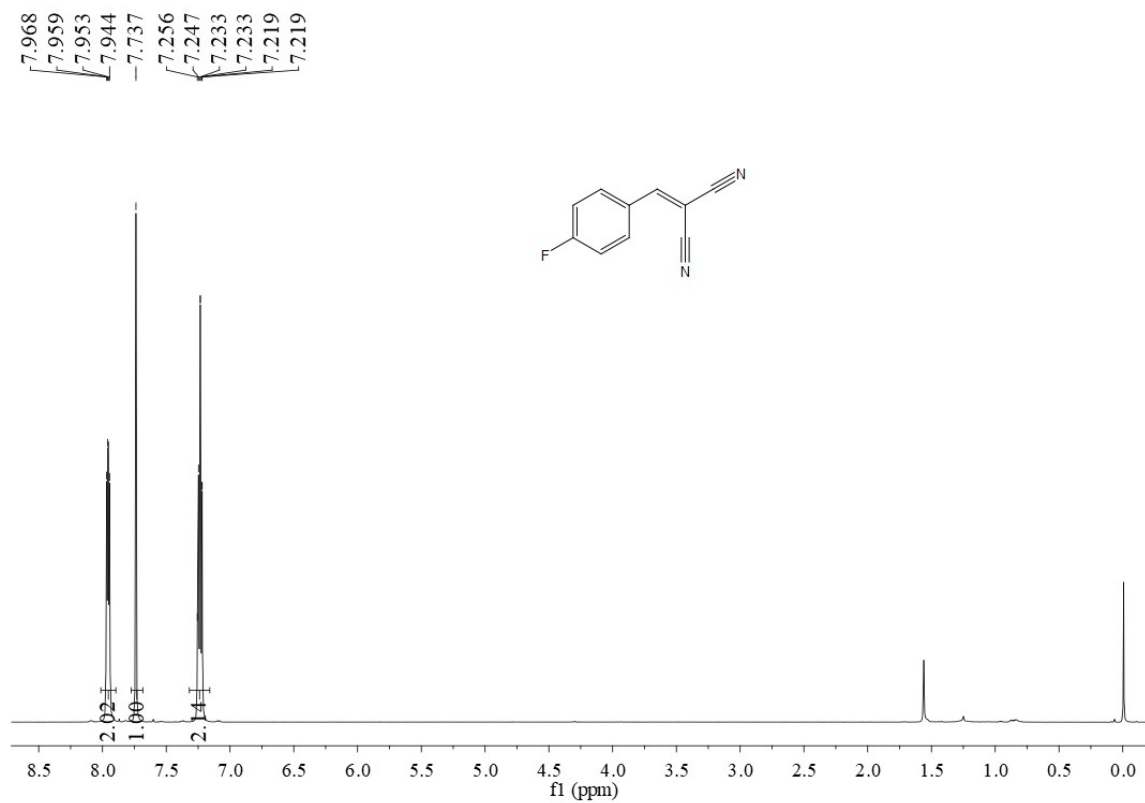


Figure S26. <sup>1</sup>H-NMR spectrum of 2b.

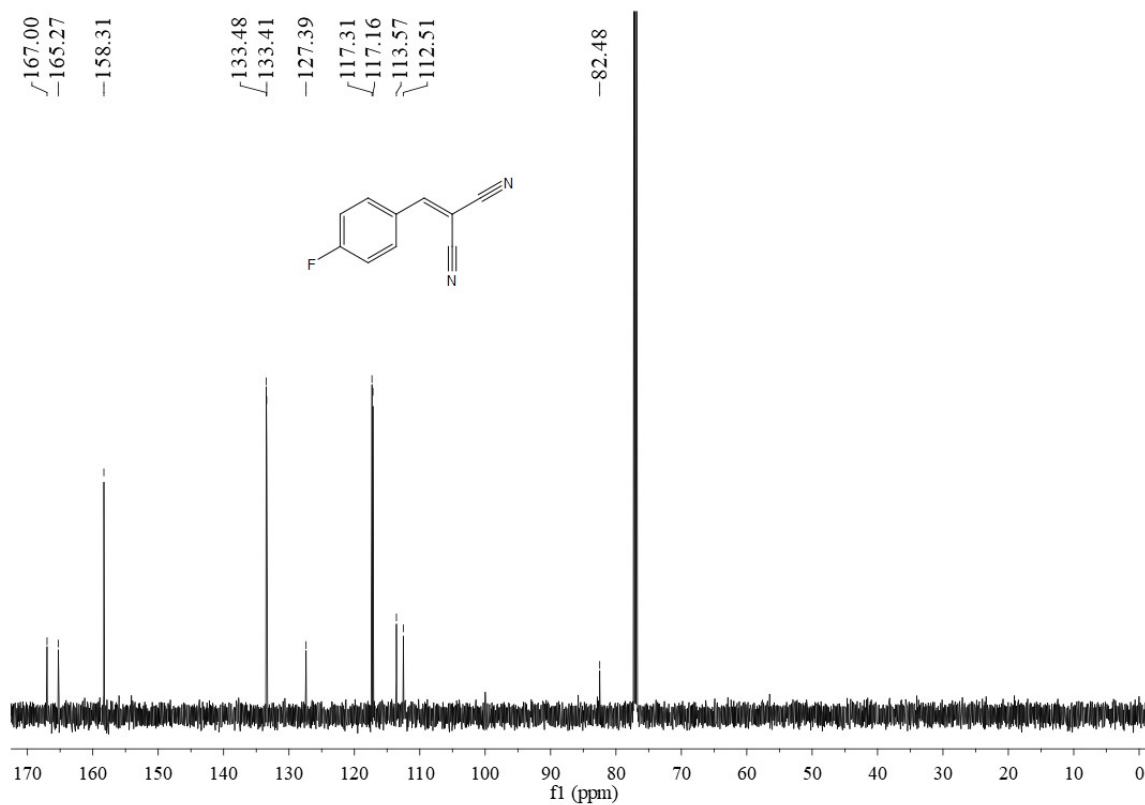


Figure S27. <sup>13</sup>C-NMR spectrum of 2b.

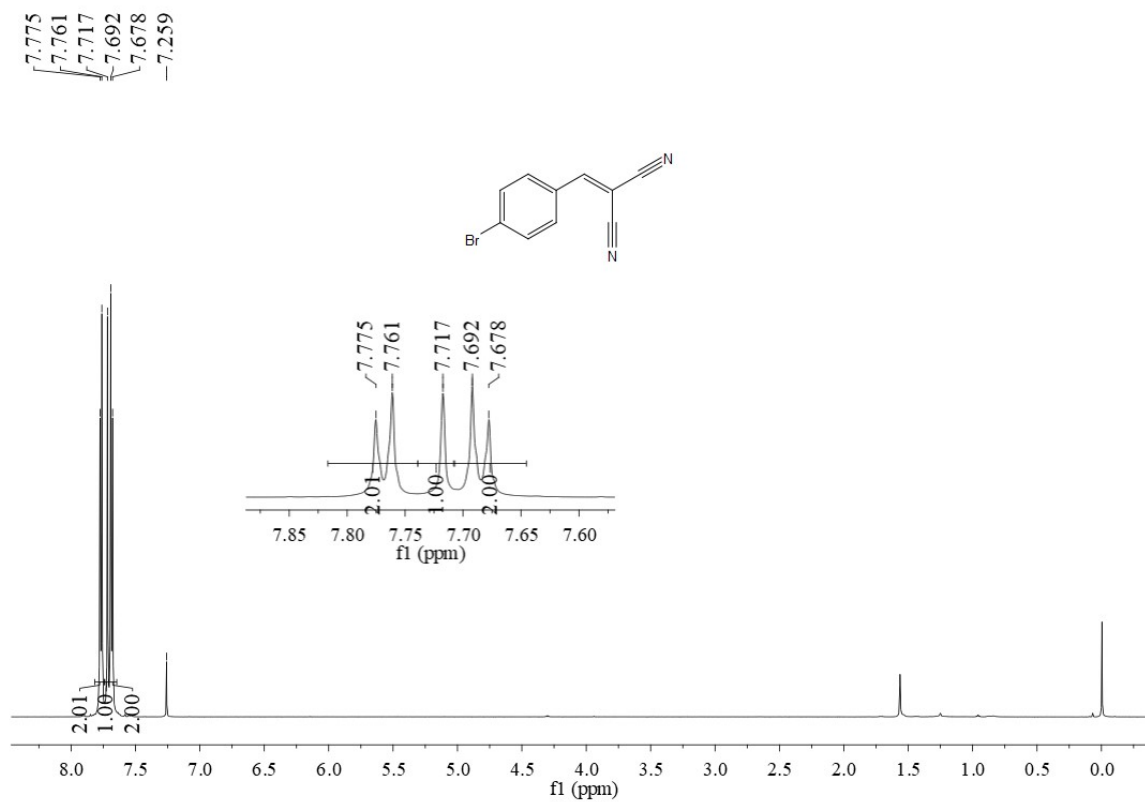


Figure S28. <sup>1</sup>H-NMR spectrum of 2c.

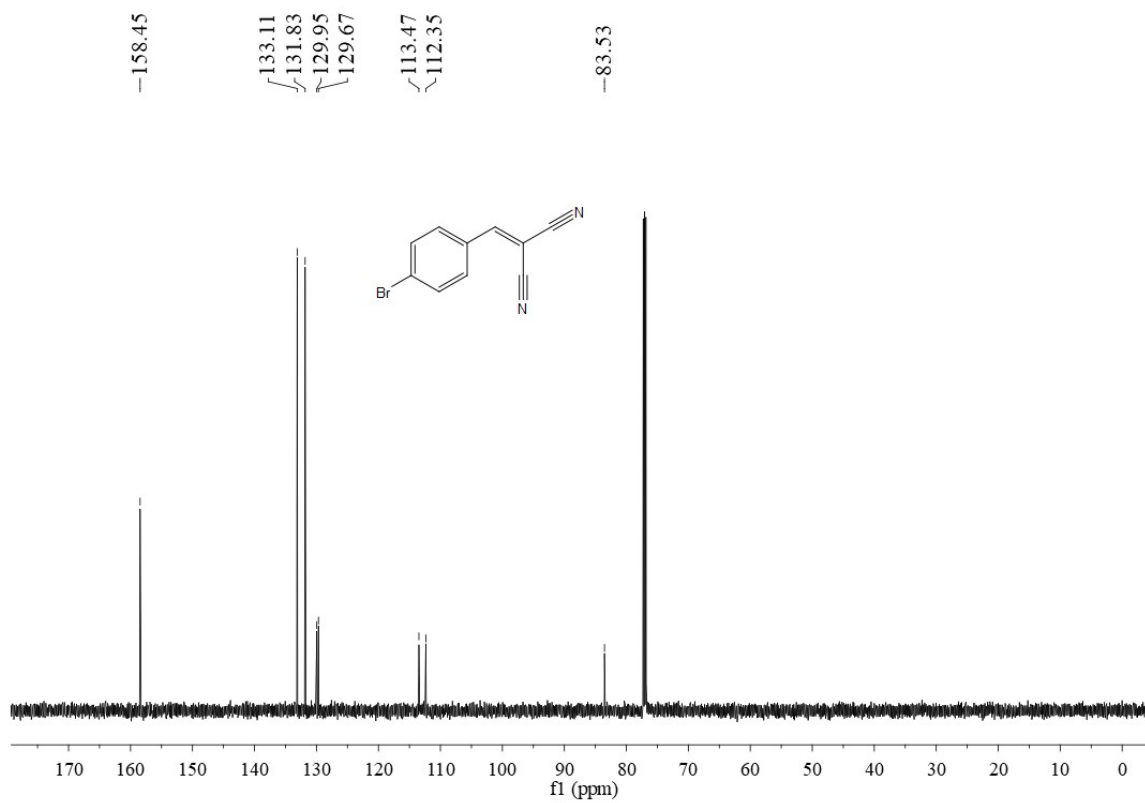


Figure S29. <sup>13</sup>C-NMR spectrum of 2c.

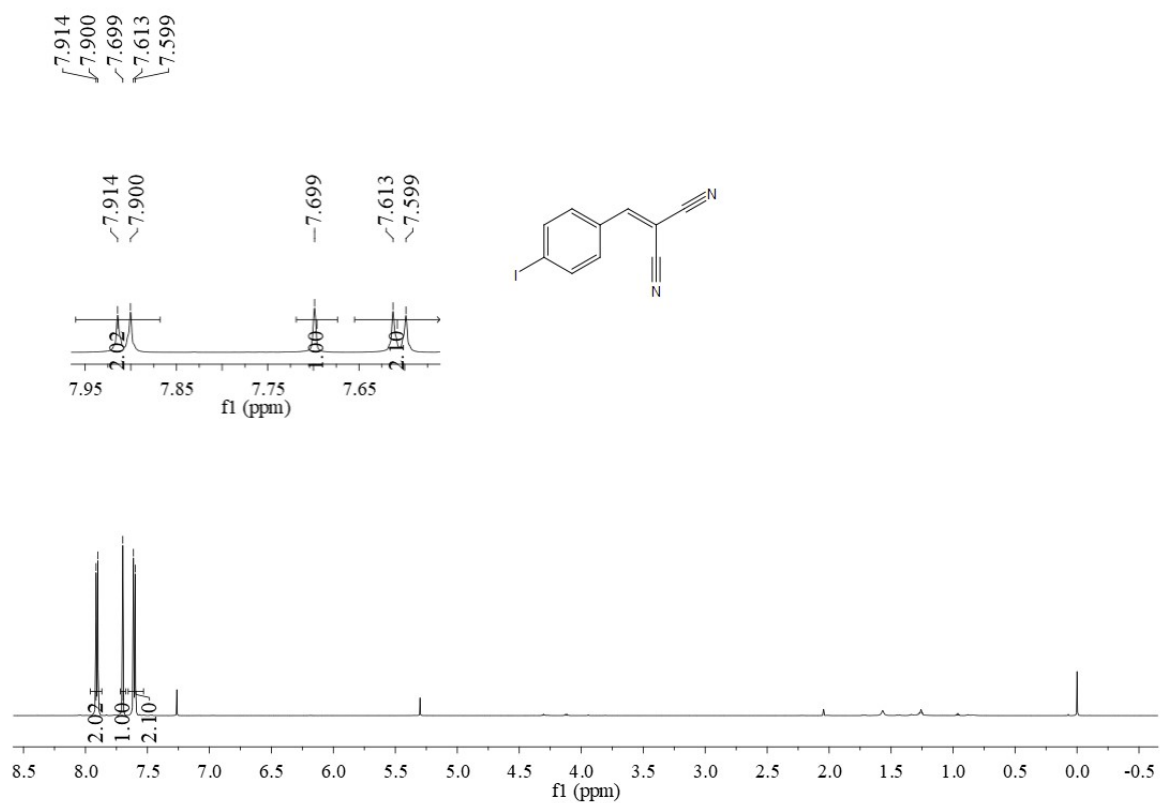


Figure S30. <sup>1</sup>H-NMR spectrum of 2d.

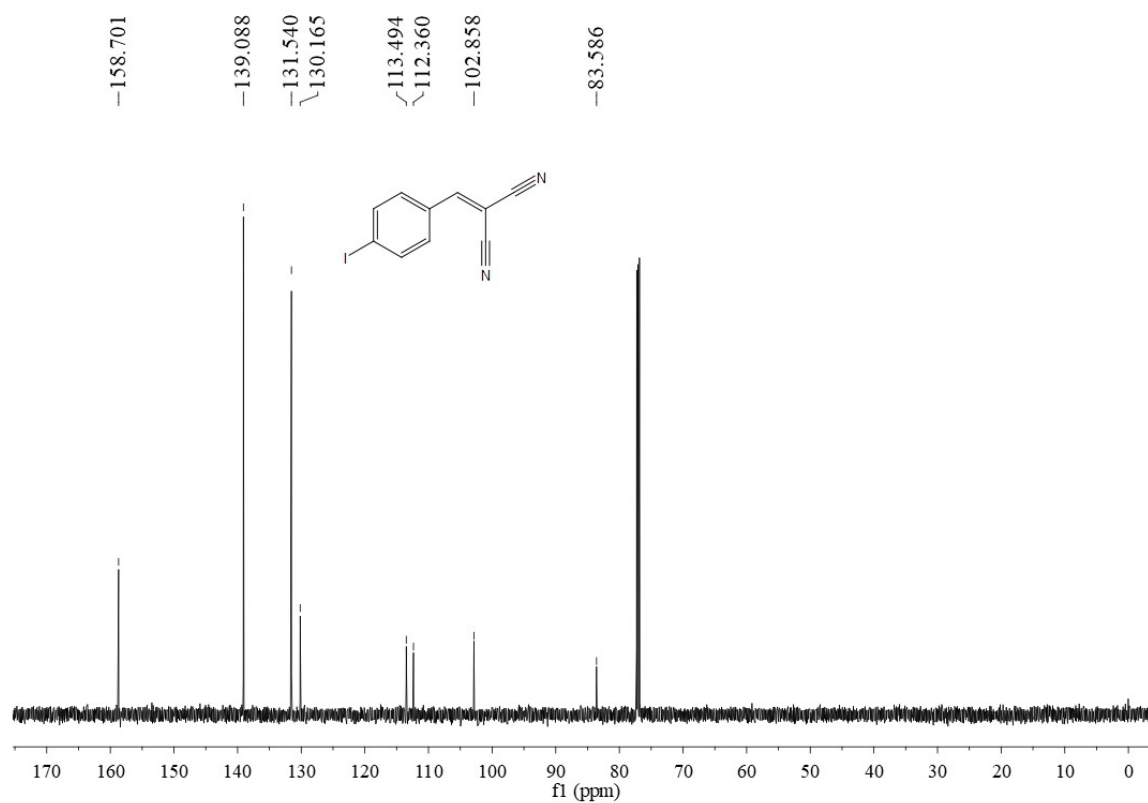


Figure S31. <sup>13</sup>C-NMR spectrum of 2d.

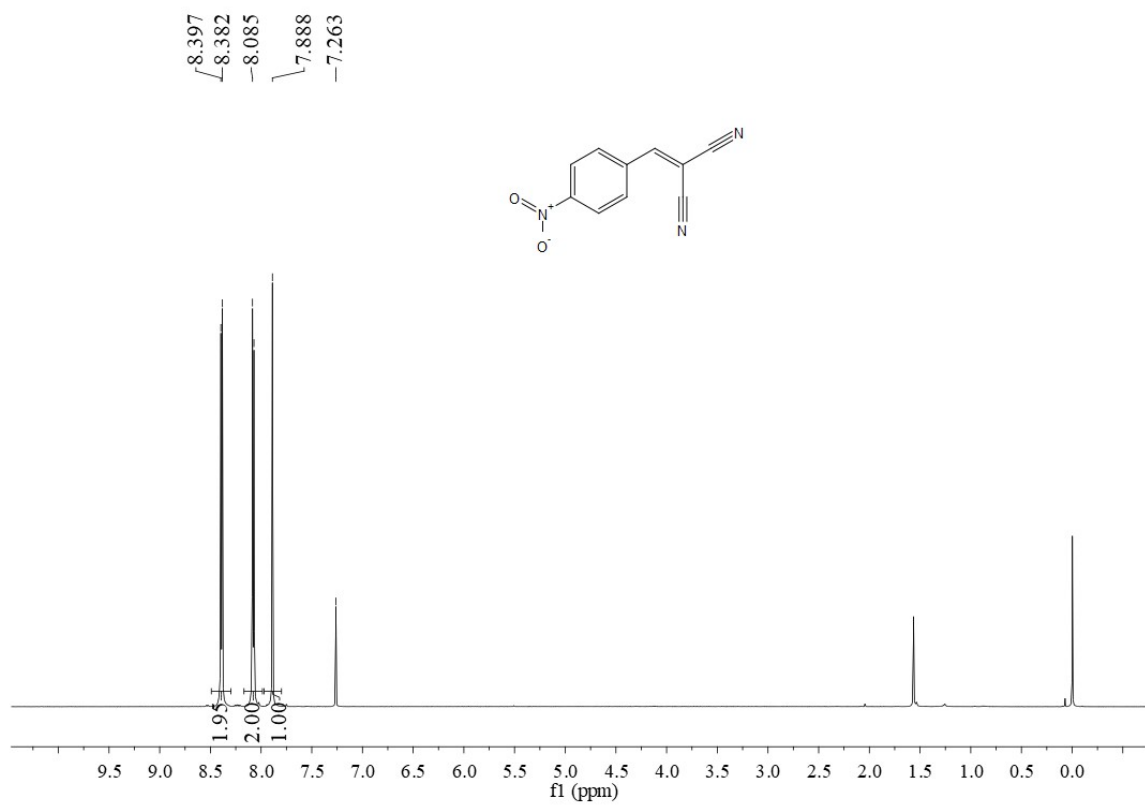


Figure S32. <sup>1</sup>H-NMR spectrum of 2e.

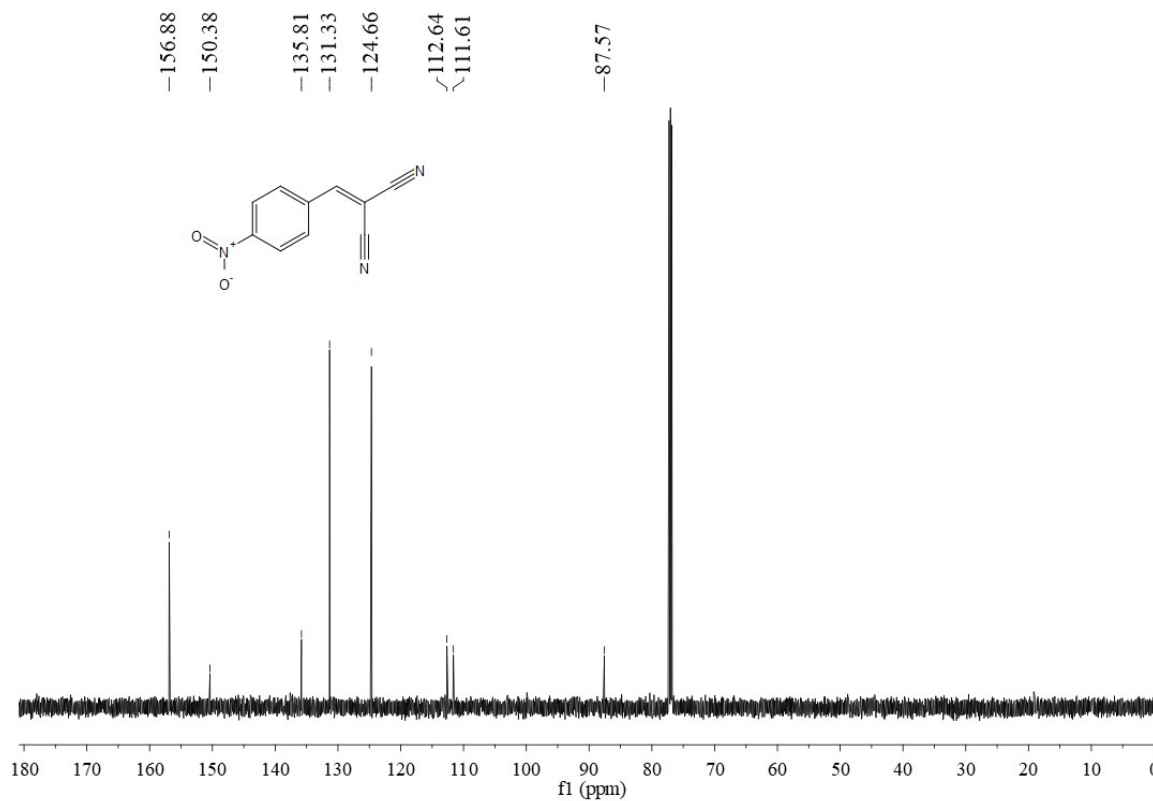


Figure S33. <sup>13</sup>C-NMR spectrum of 2e.

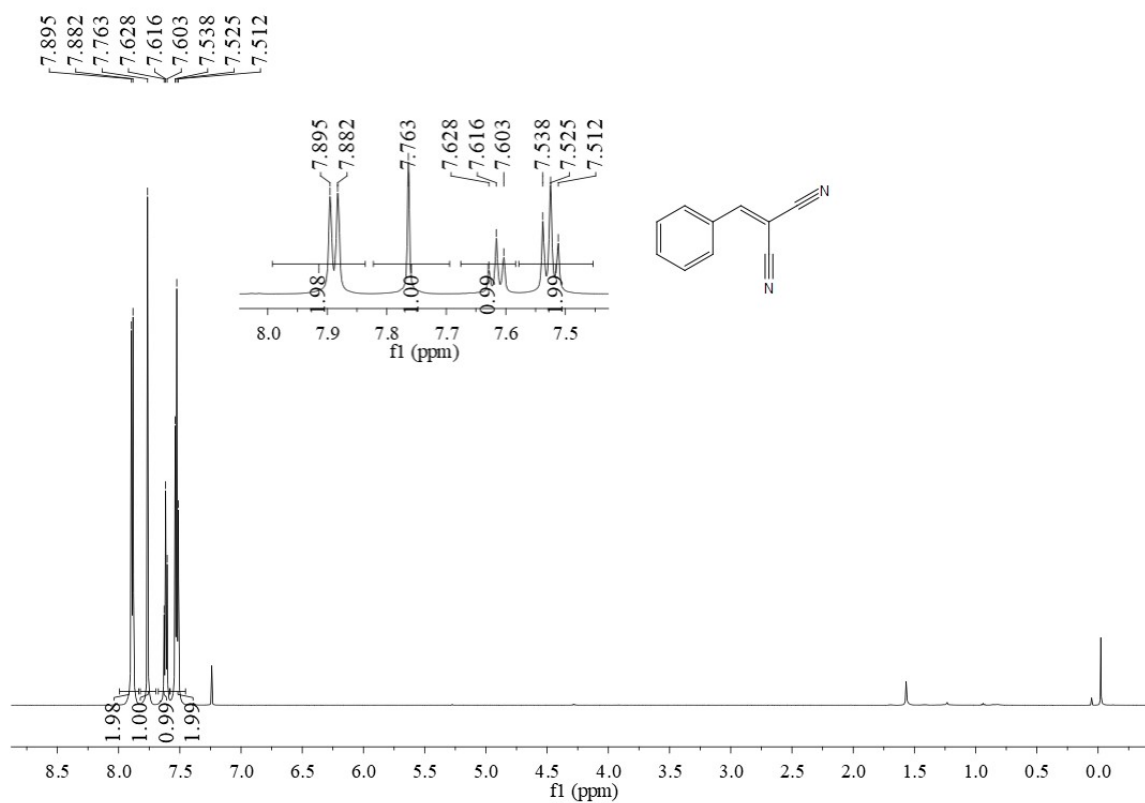


Figure S34.  $^1\text{H}$ -NMR spectrum of 2f.

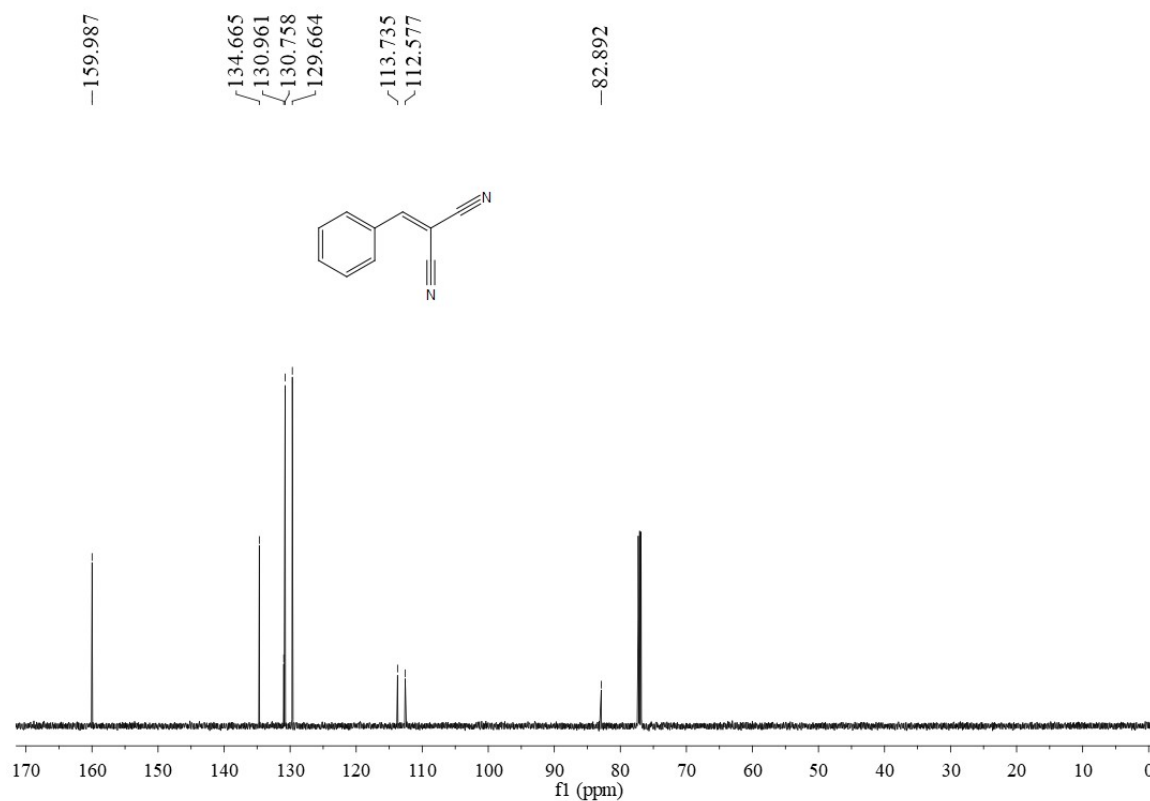


Figure S35.  $^{13}\text{C}$ -NMR spectrum of 2f.



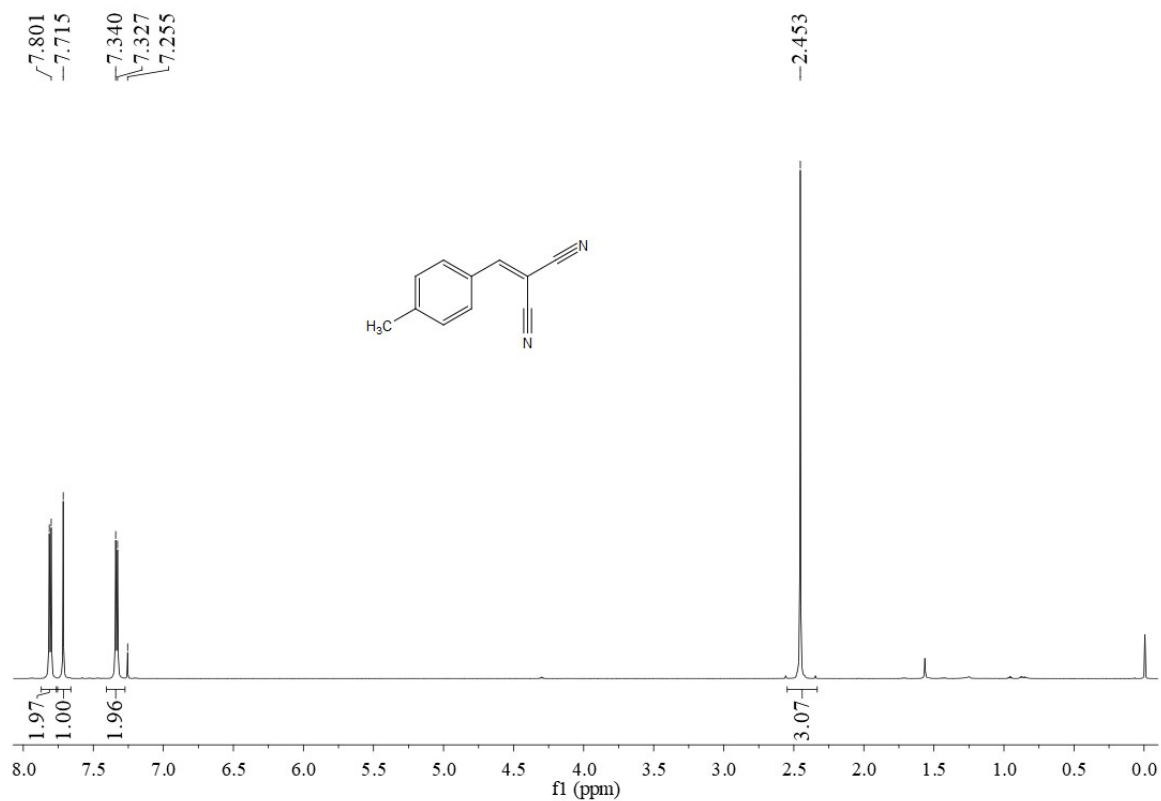


Figure S36. <sup>1</sup>H-NMR spectrum of **2g**.

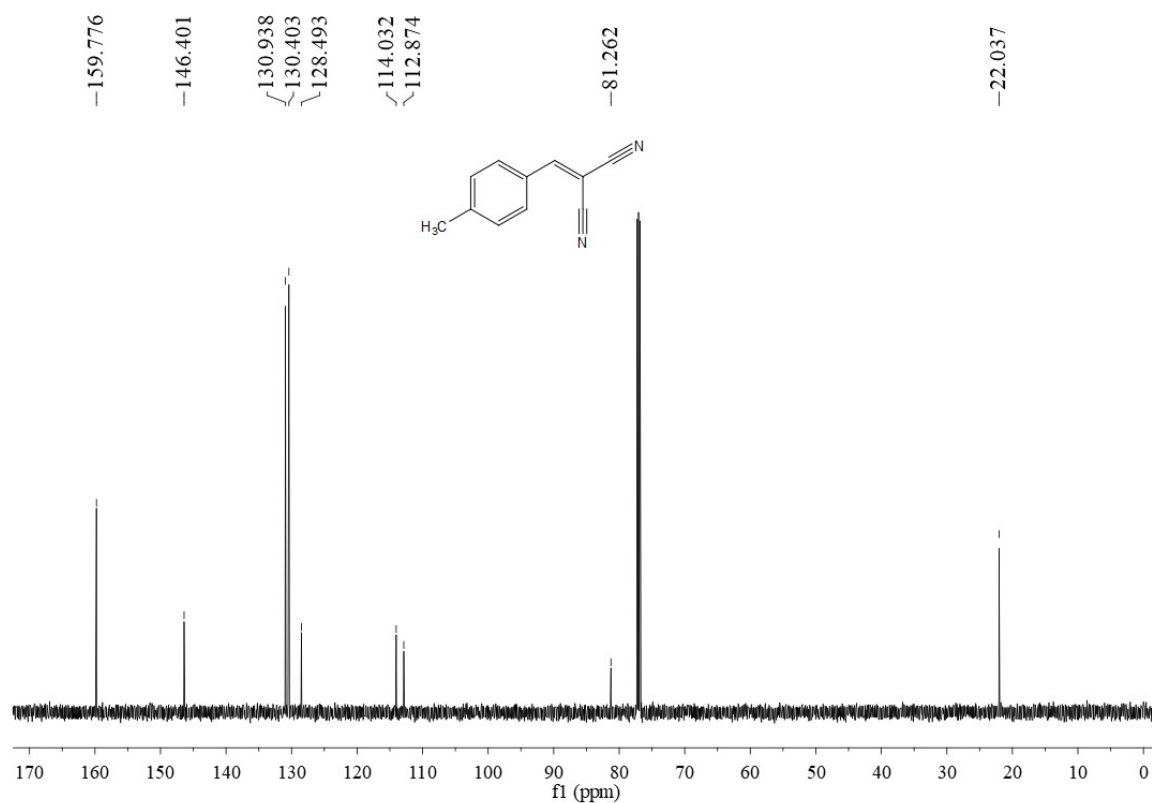


Figure S37. <sup>13</sup>C-NMR spectrum of **2g**.

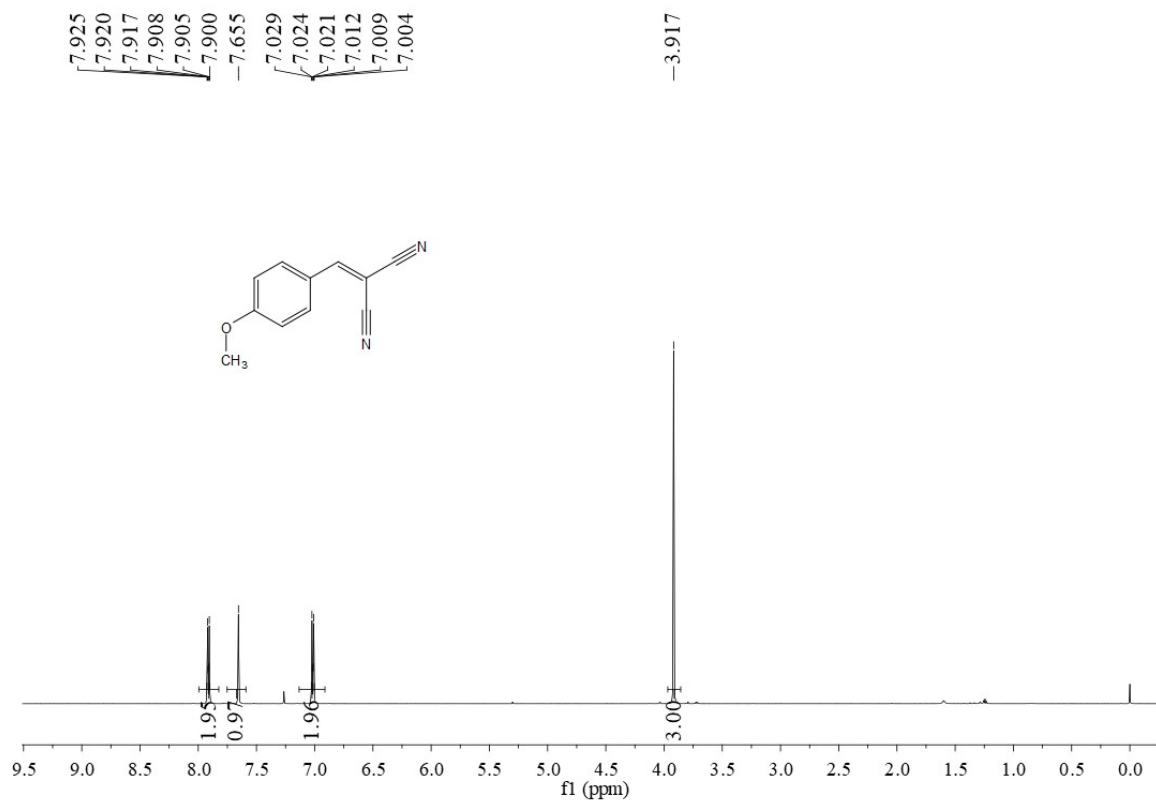


Figure S38. <sup>1</sup>H-NMR spectrum of 2h.

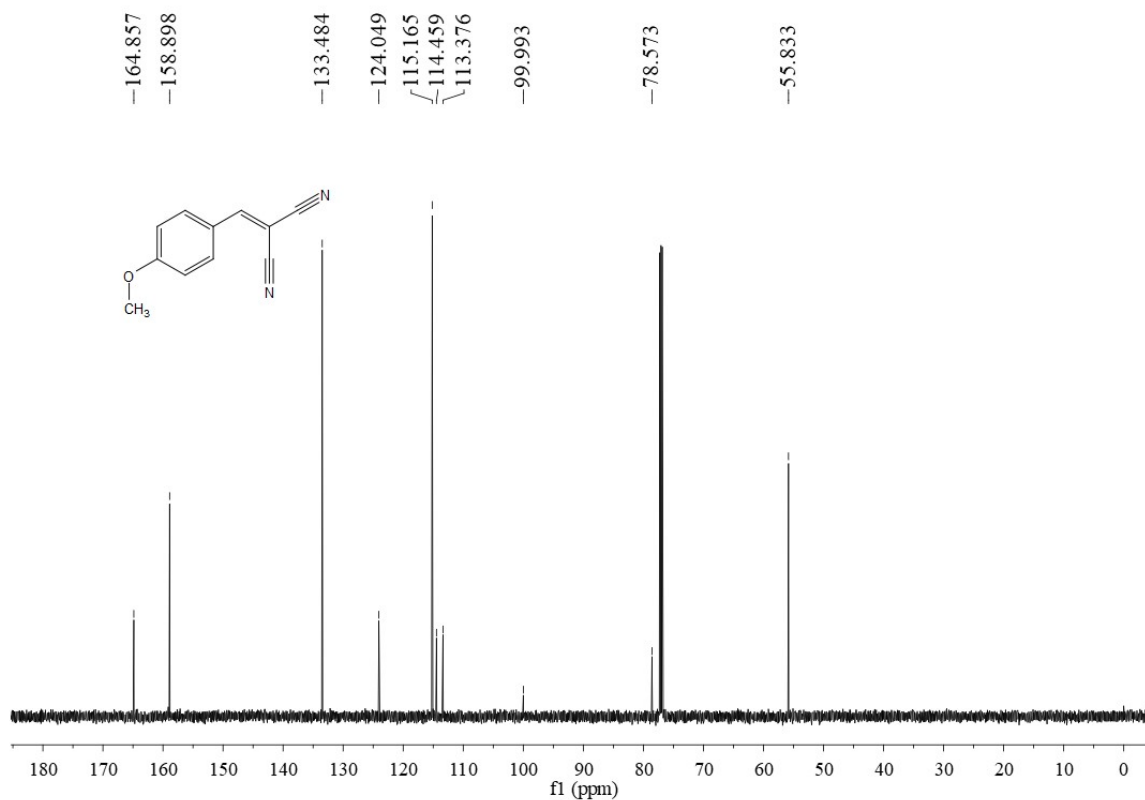


Figure S39. <sup>13</sup>C-NMR spectrum of 2h.

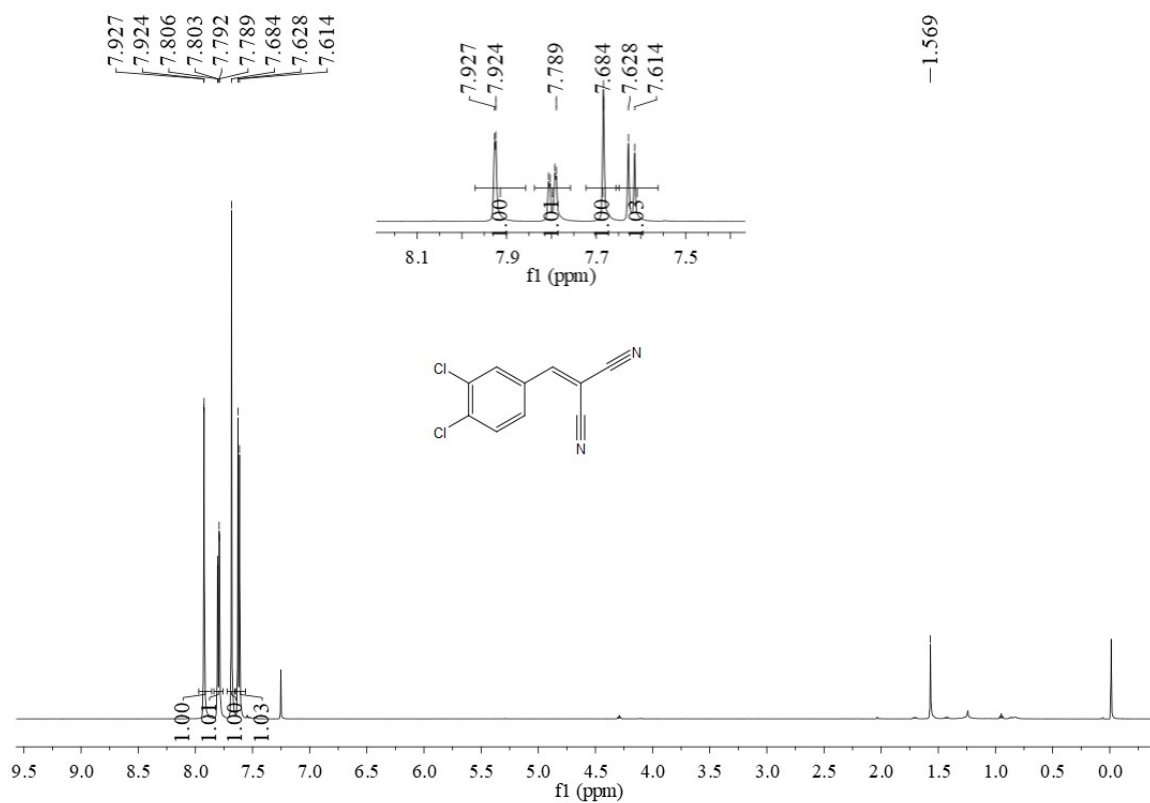


Figure S40. <sup>1</sup>H-NMR spectrum of 2i.

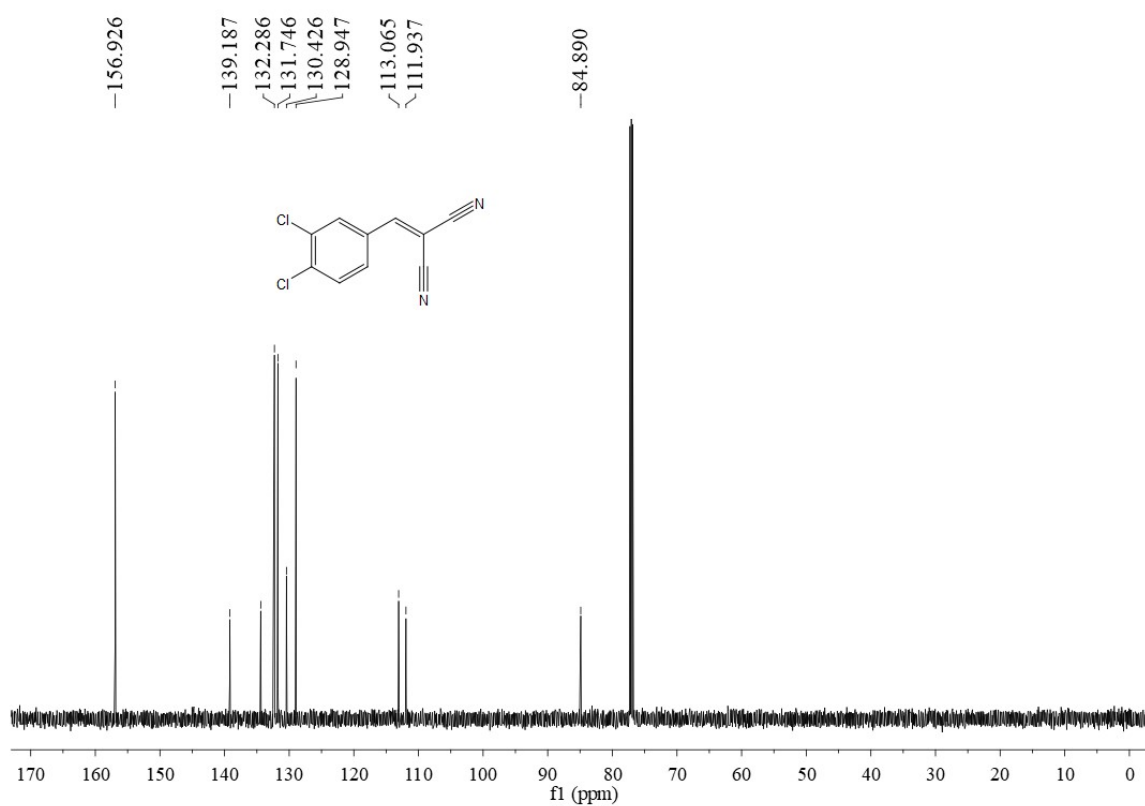


Figure S41. <sup>13</sup>C-NMR spectrum of 2i.

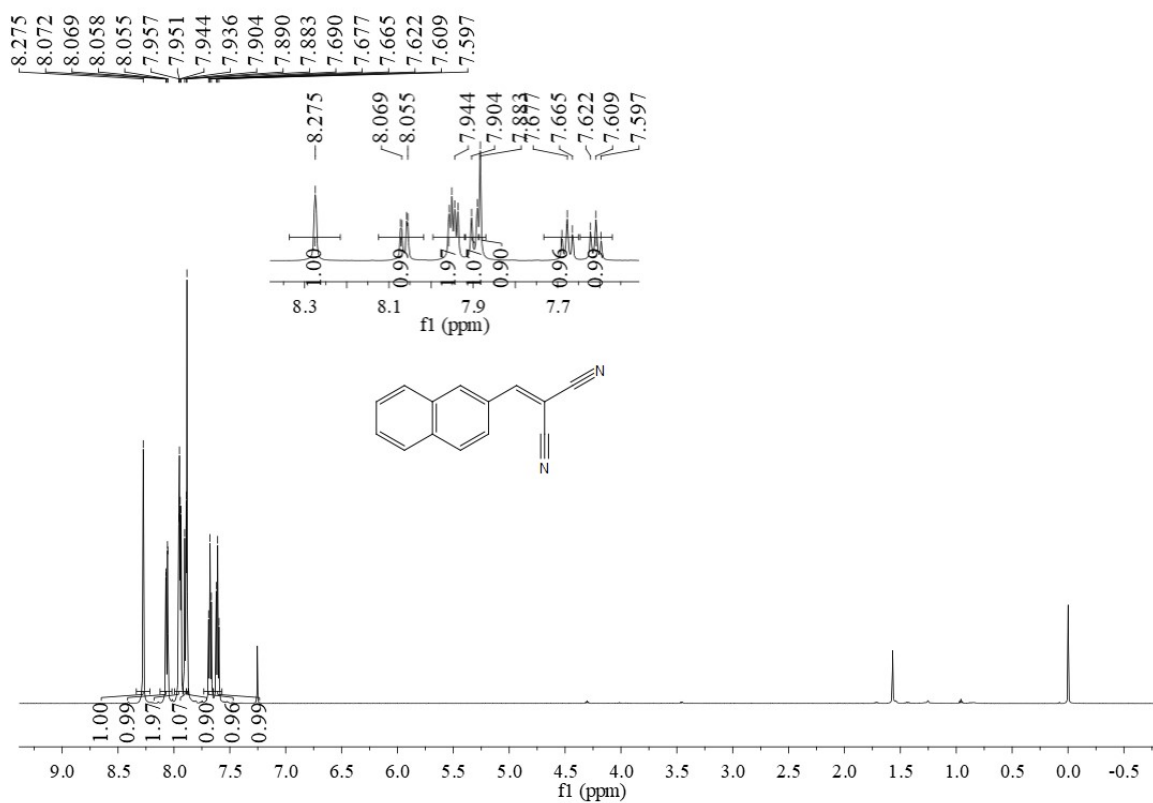


Figure S42. <sup>1</sup>H-NMR spectrum of 2j.

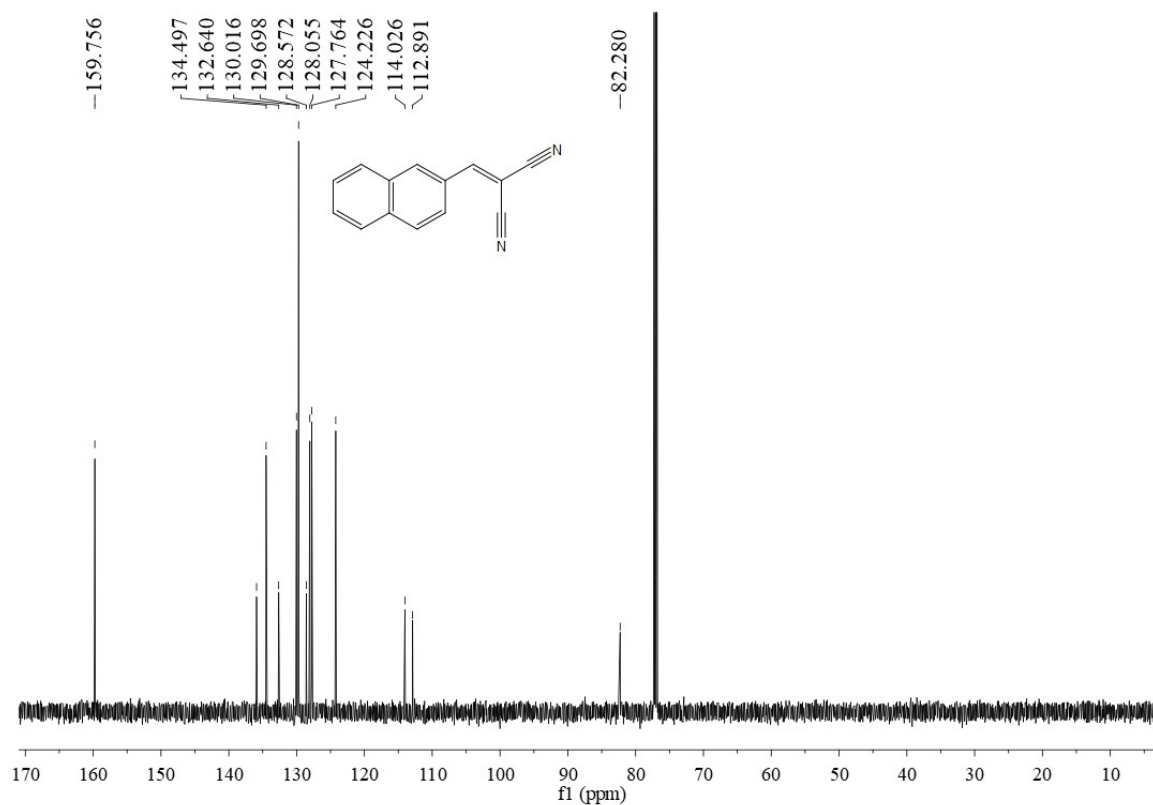


Figure S43. <sup>13</sup>C-NMR spectrum of 2j.

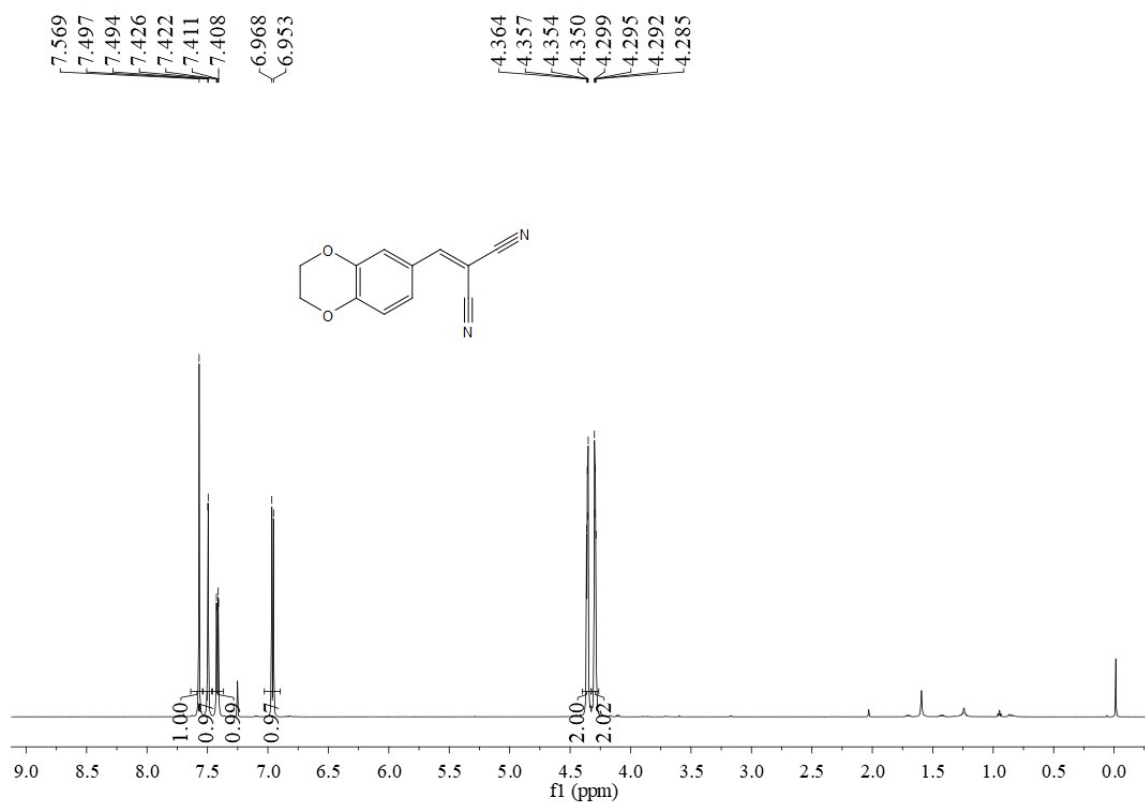


Figure S44. <sup>1</sup>H-NMR spectrum of 2k.

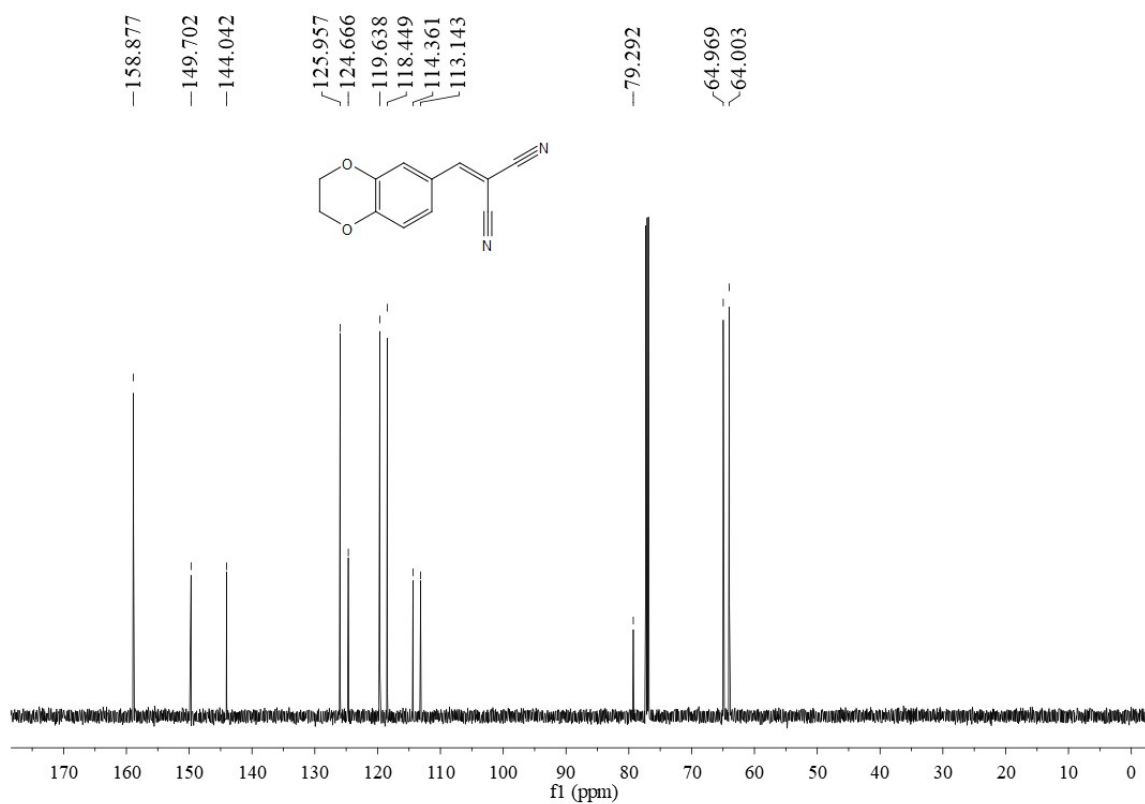


Figure S45. <sup>13</sup>C-NMR spectrum of 2k.

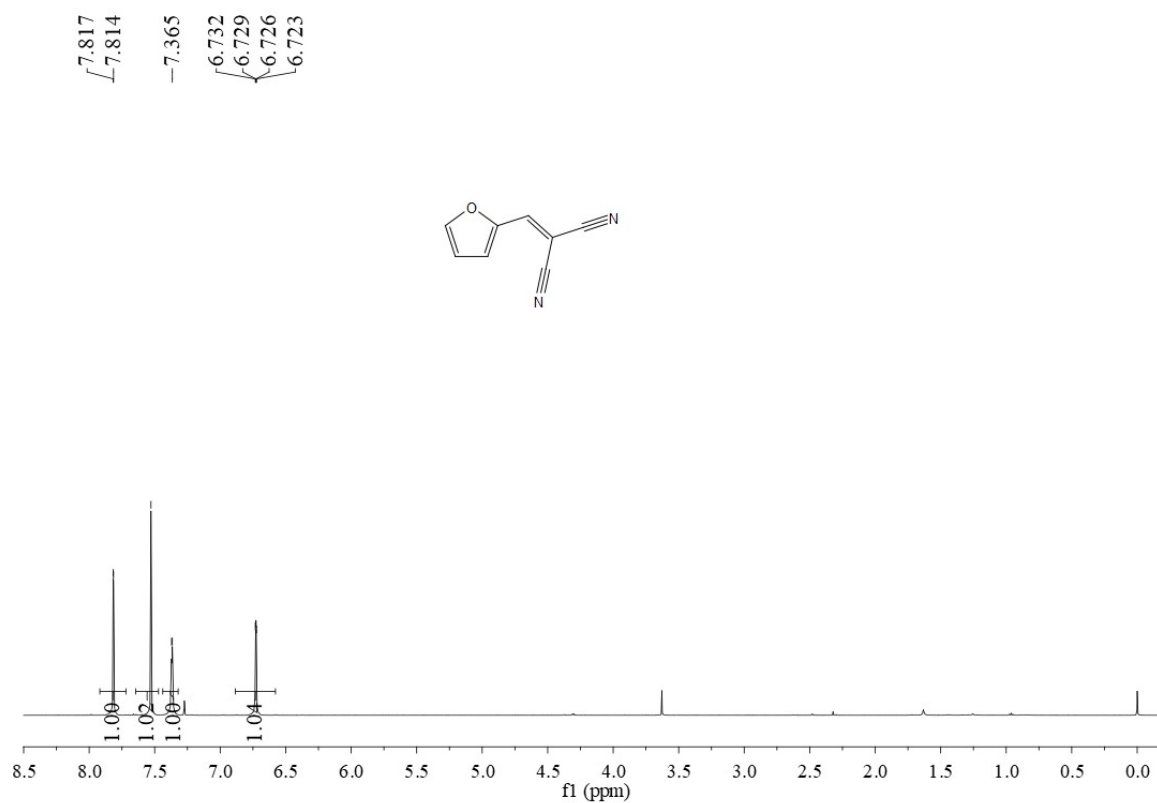


Figure S46.  $^1\text{H}$ -NMR spectrum of 2l.

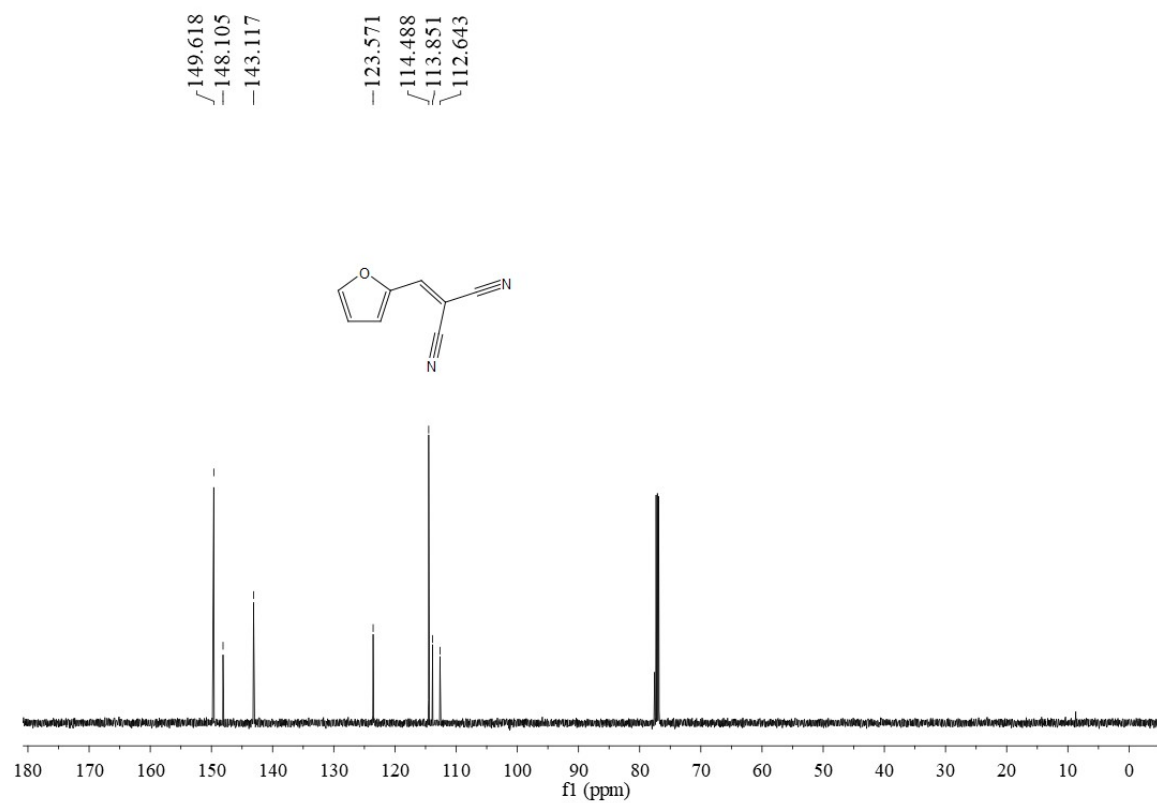


Figure S47.  $^{13}\text{C}$ -NMR spectrum of 2l.

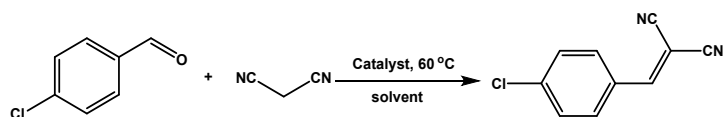
## Section C. Supporting Tables

**Table S1.** Optimization of synthesis conditions for TP-TU-COF

Entry	Solvents	Temperature (°C)	Crystallinity
1	NMP/TCB=2/3	90	No
2	NMP/TCB=1/4	90	No
3	<i>n</i> -BuOH/TCB=1:1	90	No
4	NMP/TCB=2/3	120	Low
5	NMP/TCB=1/4	120	No
6	NMP/TCB=3/2	180	Low
7	NMP/TCB=3/2	120	Moderate
8	NMP/TCB=3/2	150	High

**Table S2.** Elemental analysis of TP-TU-COF, TP-DMTU-COF, and TP-DMPTU-COF.

		C (%)	H (%)	N (%)	S (%)
TP-TU-COF	Calcd.	56.07	4.67	13.08	14.95
	Found	55.87	4.72	12.94	14.23
TP-DMTU-COF	Calcd.	57.89	5.26	12.28	14.04
	Found	57.21	4.92	11.83	13.76
TP-DMPTU-COF	Calcd.	62.92	5.62	10.49	11.99
	Found	62.13	5.27	10.02	11.28

**Table S3.** Screening of the reaction conditions [a].

entry	catalyst	solvent	yield (%) [b]
1	no	toluene	trace
2	TP-DMPTU-COF	toluene	89%
3	TP-DMPTU-COF	THF	40%
4	TP-DMPTU-COF	acetonitrile	52%
5	TP-DMPTU-COF	1, 4-dioxane	63%
6	TP-DMPTU-COF	DCE	47%
7	TP-DMPTU-COF	DMF	78%
8 <sup>c</sup>	TP-DMPTU-COF	toluene: H <sub>2</sub> O	98%
9 <sup>c</sup>	TP-DMTU-COF	toluene: H <sub>2</sub> O	95%
10 <sup>c</sup>	TP-TU-COF	toluene: H <sub>2</sub> O	97%

[a] Unless otherwise noted, the reaction was performed with 2 mol % of catalyst (TP-DMPTU-COF: 7.8 mg; TP-DMTU-COF: 7.0 mg; TP-TU-COF: 6.2 mg), aldehydes (0.3 mmol) and malononitrile (0.45 mmol, 1.5 equiv) in solvent (2.0 mL) at 60 °C for 10 h. [b] Yield of the isolated product. [c] toluene: H<sub>2</sub>O = 5:1 (2 ml: 0.4 ml).



**Table S4.** Atomistic coordinates for the AA-stacking mode of TP-TU-COF optimized using DFTB+ method. Lattice type: hexagonal, Space group: P6/M;  $\alpha = \beta = 90^\circ$ ,  $\gamma = 120^\circ$ ,  $a = 21.7621 \text{ \AA}$ ,  $b = 21.7621 \text{ \AA}$ ,  $c = 3.4854 \text{ \AA}$ .

C1	C	0.74257	-0.63919	0.5	0	Uiso	1
C2	C	0.71546	-0.58909	0.5	0	Uiso	1
C3	C	0.75692	-0.5181	0.5	0	Uiso	1
N4	N	0.83166	-0.4859	0.5	0	Uiso	1
C5	C	0.88517	-0.41281	0.5	0	Uiso	1
N6	N	0.95808	-0.39506	0.5	0	Uiso	1
S7	S	0.86743	-0.3576	0.5	0	Uiso	1
C8	C	0.98005	-0.44739	0.5	0	Uiso	1
C9	C	0.93143	-0.5198	0.5	0	Uiso	1
C10	C	0.95032	-0.57234	0.5	0	Uiso	1
O11	O	0.80515	-0.61798	0.5	0	Uiso	1
H12	H	0.73188	-0.48294	0.5	0	Uiso	1
H13	H	0.85695	-0.51931	0.5	0	Uiso	1
H14	H	1.00081	-0.33859	0.5	0	Uiso	1
H15	H	0.87209	-0.5393	0.5	0	Uiso	1
H16	H	0.90738	-0.63071	0.5	0	Uiso	1

**Table S5.** Atomistic coordinates for the AB-stacking mode of TP-TU-COF optimized using DFTB+ method. Lattice type: hexagonal, Space group: P63/M;  $\alpha = \beta = 90^\circ$ ,  $\gamma = 120^\circ$ ,  $a = 21.7621 \text{ \AA}$ ,  $b = 21.7621 \text{ \AA}$ ,  $c = 6.9709 \text{ \AA}$ .

C1	C	1.07591	1.02748	0.25	0	Uiso	1
C2	C	1.0488	1.07758	0.25	0	Uiso	1
C3	C	1.09026	1.14857	0.25	0	Uiso	1
N4	N	1.16499	1.18077	0.25	0	Uiso	1
C5	C	1.21851	1.25386	0.25	0	Uiso	1
N6	N	1.29142	1.27161	0.25	0	Uiso	1
S7	S	1.20076	1.30907	0.25	0	Uiso	1
C8	C	1.31338	1.21928	0.25	0	Uiso	1
C9	C	1.26476	1.14687	0.25	0	Uiso	1
C10	C	1.28365	1.09432	0.25	0	Uiso	1
O11	O	1.13849	1.04869	0.25	0	Uiso	1
H12	H	1.06521	1.18373	0.25	0	Uiso	1
H13	H	1.19028	1.14735	0.25	0	Uiso	1
H14	H	0.33414	1.32808	0.25	0	Uiso	1
H15	H	1.20542	1.12737	0.25	0	Uiso	1
H16	H	1.24072	1.03596	0.25	0	Uiso	1
C17	C	0.59076	1.30586	0.25	0	Uiso	1
C18	C	0.61787	1.25575	0.25	0	Uiso	1
C19	C	0.57641	1.18476	0.25	0	Uiso	1
N20	N	0.50168	1.15257	0.25	0	Uiso	1
C21	C	0.44816	1.07947	0.25	0	Uiso	1
N22	N	0.37525	1.06173	0.25	0	Uiso	1
S23	S	0.46591	1.02426	0.25	0	Uiso	1
C24	C	0.35329	1.11406	0.25	0	Uiso	1
C25	C	0.40191	1.18647	0.25	0	Uiso	1
C26	C	0.38302	1.23901	0.25	0	Uiso	1
O27	O	0.52818	1.28465	0.25	0	Uiso	1
H28	H	0.60146	1.1496	0.25	0	Uiso	1
H29	H	0.47638	1.18598	0.25	0	Uiso	1
H30	H	1.33252	1.00526	0.25	0	Uiso	1
H31	H	0.46124	1.20596	0.25	0	Uiso	1
H32	H	0.42595	1.29738	0.25	0	Uiso	1

**Table S6.** Atomistic coordinates for the AA-stacking mode of TP-DMTU-COF optimized using DFTB<sup>+</sup> method. Lattice type: hexagonal, Space group: P6;  $\alpha = \beta = 90^\circ$ ,  $\gamma = 120^\circ$ , a = 21.8507 Å, b = 21.8507 Å, c = 3.5805 Å.

C1	C	0.74263	0.36735	0.234	0	Uiso	1
C2	C	0.70892	0.41051	0.28603	0	Uiso	1
C3	C	0.74531	0.47991	0.35391	0	Uiso	1
N4	N	0.8139	0.51237	0.51745	0	Uiso	1
C5	C	0.87311	0.57596	0.39347	0	Uiso	1
N6	N	0.94212	0.59285	0.51707	0	Uiso	1
S7	S	0.86267	0.63118	0.2442	0	Uiso	1
C8	C	0.97026	0.54523	0.55565	0	Uiso	1
C9	C	0.92803	0.4713	0.57576	0	Uiso	1
C10	C	0.9567	0.42652	0.59777	0	Uiso	1
O11	O	0.80238	0.39344	0.11315	0	Uiso	1
C12	C	0.08971	0.64969	0.70895	0	Uiso	1
H13	H	0.72046	0.51114	0.31562	0	Uiso	1
H14	H	0.97713	0.64702	0.53551	0	Uiso	1
H15	H	0.87297	0.44704	0.59588	0	Uiso	1
H16	H	0.81842	0.49472	0.77808	0	Uiso	1
H17	H	0.09842	0.68728	0.48359	0	Uiso	1
H18	H	0.14154	0.66018	0.81252	0	Uiso	1
H19	H	0.06322	0.66206	0.93317	0	Uiso	1

**Table S7.** Atomistic coordinates for the AB-stacking mode of TP-DMTU-COF optimized using DFTB<sup>+</sup> method. Lattice type: hexagonal, Space group: P63;  $\alpha = \beta = 90^\circ$ ,  $\gamma = 120^\circ$ ,  $a = 21.8507 \text{ \AA}$ ,  $b = 21.8507 \text{ \AA}$ ,  $c = 7.1610 \text{ \AA}$ .

C1	C	1.07597	0.03402	0.117	0	Uiso	1
C2	C	1.04225	0.07718	0.14302	0	Uiso	1
C3	C	1.07864	0.14658	0.17696	0	Uiso	1
N4	N	1.14724	0.17904	0.25872	0	Uiso	1
C5	C	1.20644	0.24263	0.19674	0	Uiso	1
N6	N	1.27545	0.25952	0.25854	0	Uiso	1
S7	S	1.196	0.29785	0.1221	0	Uiso	1
C8	C	1.30359	0.21189	0.27782	0	Uiso	1
C9	C	1.26136	0.13797	0.28788	0	Uiso	1
C10	C	1.29003	0.09318	0.29889	0	Uiso	1
O11	O	1.13572	0.06011	0.05657	0	Uiso	1
C12	C	0.42305	0.31635	0.35447	0	Uiso	1
H13	H	1.05379	0.17781	0.15781	0	Uiso	1
H14	H	1.31046	0.31369	0.26775	0	Uiso	1
H15	H	1.2063	0.11371	0.29794	0	Uiso	1
H16	H	1.15176	0.16139	0.38904	0	Uiso	1
H17	H	0.43176	0.35395	0.24179	0	Uiso	1
H18	H	0.47487	0.32684	0.40626	0	Uiso	1
H19	H	0.39656	0.32873	0.46659	0	Uiso	1
C20	C	0.5907	0.29931	0.117	0	Uiso	1
C21	C	0.62441	0.25615	0.14302	0	Uiso	1
C22	C	0.58802	0.18675	0.17696	0	Uiso	1
N23	N	0.51943	0.15429	0.25872	0	Uiso	1
C24	C	0.46023	0.09071	0.19674	0	Uiso	1
N25	N	0.39121	0.07381	0.25854	0	Uiso	1
S26	S	0.47067	0.03548	0.1221	0	Uiso	1
C27	C	0.36307	0.12144	0.27782	0	Uiso	1
C28	C	0.40531	0.19536	0.28788	0	Uiso	1
C29	C	0.37664	0.24015	0.29889	0	Uiso	1
O30	O	0.53095	0.27323	0.05657	0	Uiso	1
C31	C	1.24362	0.01698	0.35447	0	Uiso	1
H32	H	0.61287	0.15552	0.15781	0	Uiso	1
H33	H	0.35621	0.01964	0.26775	0	Uiso	1
H34	H	0.46036	0.21963	0.29794	0	Uiso	1
H35	H	0.51491	0.17194	0.38904	0	Uiso	1
H36	H	1.23491	0.02061	0.24179	0	Uiso	1

H37	H	1.1918	0.00649	0.40626	0	Uiso	1
H38	H	1.27011	0.0046	0.46659	0	Uiso	1

**Table S8.** Atomistic coordinates for the AA-stacking mode of TP-DMPTU-COF optimized using DFTB<sup>+</sup> method. Lattice type: hexagonal, Space group: P6;  $\alpha = \beta = 90^\circ$ ,  $\gamma = 120^\circ$ , a = 28.6367 Å, b = 28.6367 Å, c = 3.6239 Å.

C1	C	-0.36821	0.35731	0.55747	0	Uiso	1
C2	C	-0.30909	0.39303	0.60294	0	Uiso	1
C3	C	-0.28352	0.44679	0.6667	0	Uiso	1
N4	N	-0.30621	0.48215	0.64572	0	Uiso	1
C5	C	-0.27712	0.53427	0.46332	0	Uiso	1
N6	N	-0.30174	0.56714	0.41667	0	Uiso	1
S7	S	-0.22058	0.55786	0.37425	0	Uiso	1
C8	C	-0.35874	0.54701	0.41227	0	Uiso	1
C9	C	-0.39353	0.49546	0.28387	0	Uiso	1
C10	C	-0.44909	0.47646	0.24904	0	Uiso	1
C11	C	-0.47042	0.51006	0.34371	0	Uiso	1
C12	C	-0.43505	0.56219	0.47359	0	Uiso	1
C13	C	-0.37967	0.58092	0.50914	0	Uiso	1
O14	O	-0.39716	0.37494	0.45482	0	Uiso	1
H15	H	-0.24069	0.46589	0.7149	0	Uiso	1
H16	H	-0.34421	0.47019	0.75909	0	Uiso	1
H17	H	-0.27635	0.6072	0.35187	0	Uiso	1
H18	H	-0.37342	0.46879	0.23871	0	Uiso	1
H19	H	-0.47486	0.43554	0.15159	0	Uiso	1
H20	H	-0.45106	0.5876	0.56025	0	Uiso	1
C21	C	-0.34369	0.63648	0.66252	0	Uiso	1
H22	H	-0.36747	0.65181	0.80775	0	Uiso	1
H23	H	-0.32021	0.66487	0.43981	0	Uiso	1
H24	H	-0.3153	0.63448	0.86	0	Uiso	1

**Table S9.** Atomistic coordinates for the AB-stacking mode of TP-DMPTU-COF optimized using DFTB<sup>+</sup> method. Lattice type: hexagonal, Space group: P63;  $\alpha = \beta = 90^\circ$ ,  $\gamma = 120^\circ$ ,  $a = 28.6367 \text{ \AA}$ ,  $b = 28.6367 \text{ \AA}$ ,  $c = 7.2478 \text{ \AA}$ .

C1	C	0.9649	0.02372	0.27874	0	Uiso	1
C2	C	1.02398	0.05966	0.30147	0	Uiso	1
C3	C	1.04933	0.11342	0.33335	0	Uiso	1
N4	N	1.0264	0.14856	0.32286	0	Uiso	1
C5	C	1.05528	0.20069	0.23166	0	Uiso	1
N6	N	1.03041	0.23334	0.20834	0	Uiso	1
S7	S	1.11184	0.22453	0.18712	0	Uiso	1
C8	C	0.97337	0.21296	0.20614	0	Uiso	1
C9	C	0.93877	0.16136	0.14194	0	Uiso	1
C10	C	0.88316	0.14211	0.12452	0	Uiso	1
C11	C	0.86159	0.17551	0.17186	0	Uiso	1
C12	C	0.89678	0.22768	0.23679	0	Uiso	1
C13	C	0.9522	0.24666	0.25457	0	Uiso	1
O14	O	0.93577	0.04114	0.22741	0	Uiso	1
H15	H	1.09218	0.13269	0.35745	0	Uiso	1
H16	H	0.98836	0.13642	0.37955	0	Uiso	1
H17	H	1.05566	0.27343	0.17594	0	Uiso	1
H18	H	0.95907	0.13487	0.11935	0	Uiso	1
H19	H	0.85754	0.10116	0.07579	0	Uiso	1
H20	H	0.88059	0.25294	0.28013	0	Uiso	1
C21	C	0.98797	0.30226	0.33126	0	Uiso	1
H22	H	0.96405	0.31743	0.40387	0	Uiso	1
H23	H	1.01137	0.3307	0.2199	0	Uiso	1
H24	H	1.01645	0.30042	0.43	0	Uiso	1
C25	C	0.70176	0.30961	0.27874	0	Uiso	1
C26	C	0.64269	0.27367	0.30147	0	Uiso	1
C27	C	0.61733	0.21991	0.33335	0	Uiso	1
N28	N	0.64027	0.18478	0.32286	0	Uiso	1
C29	C	0.61138	0.13264	0.23166	0	Uiso	1
N30	N	0.63625	0.09999	0.20834	0	Uiso	1
S31	S	0.55483	0.10881	0.18712	0	Uiso	1
C32	C	0.6933	0.12037	0.20614	0	Uiso	1
C33	C	0.7279	0.17197	0.14194	0	Uiso	1
C34	C	0.78351	0.19122	0.12452	0	Uiso	1
C35	C	0.80508	0.15783	0.17186	0	Uiso	1
C36	C	0.76989	0.10565	0.23679	0	Uiso	1
C37	C	0.71446	0.08667	0.25457	0	Uiso	1

O38	O	0.73089	0.29219	0.22741	0	Uiso	1
H39	H	0.57449	0.20064	0.35745	0	Uiso	1
H40	H	0.67831	0.19691	0.37955	0	Uiso	1
H41	H	0.61101	0.0599	0.17594	0	Uiso	1
H42	H	0.70759	0.19846	0.11935	0	Uiso	1
H43	H	0.80913	0.23217	0.07579	0	Uiso	1
H44	H	0.78608	0.08039	0.28013	0	Uiso	1
C45	C	0.67869	0.03107	0.33126	0	Uiso	1
H46	H	0.70261	0.01591	0.40387	0	Uiso	1
H47	H	0.6553	0.00263	0.2199	0	Uiso	1
H48	H	0.65021	0.03291	0.43	0	Uiso	1



#### Section D. Supporting References

- [S1] C. R. Deblase, K. E. Silberstein, T. -T. Truong, H. D. Abruña, W. R. Dichtel, *J. Am. Chem. Soc.* **2013**, *135*, 16821-16824.
- [S2] M. Matsumoto, R. R. Dasari, W. Ji, C. H. Feriante, T. C. Parker, S. R. Marder, W. R. Dichtel, *J. Am. Chem. Soc.* **2017**, *139*, 4999-5002.
- [S3] E. Vitaku, W. R. Dichtel, *J. Am. Chem. Soc.* **2017**, *139*, 12911-12914.